POLITECNICO DI MILANO

1st Workshop EASN

Paris, 7-8 october 2010

Fatigue Properties of a Gamma Titanium Aluminide Alloy

S. Beretta, **M. Filippini**, L. Patriarca – Politecnico di Milano

G. Pasquero, S. Sabbadini – AVIO SpA

Introduction

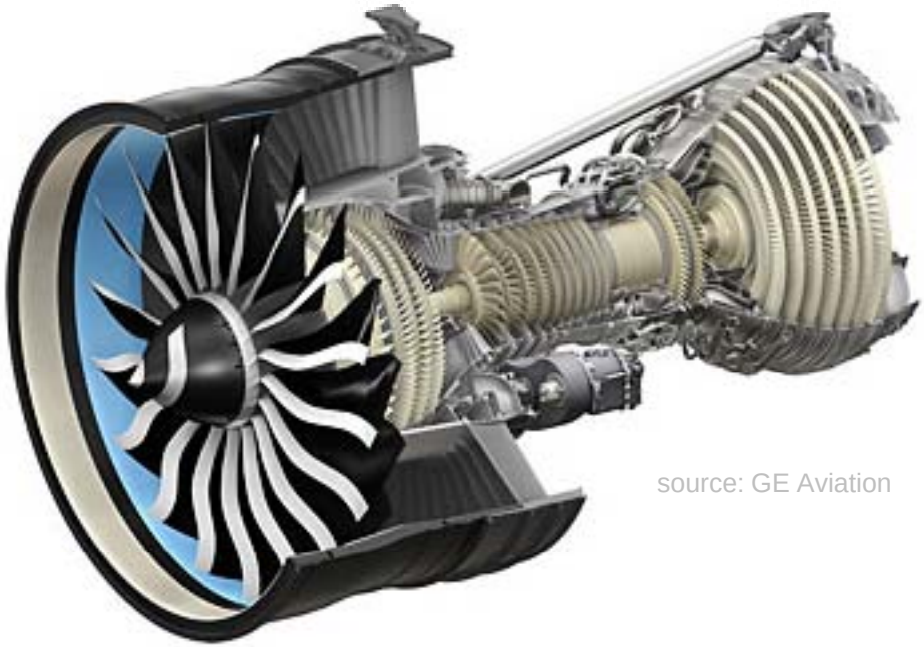

source: GE Aviation

The headline objectives of the ACARE (Advisory Council for Aeronautics Research in Europe) to be achieved through the implementation of ACARE's SRA (Strategic Research Agenda) include, among other things, 50% and 80% cuts in CO_2 and NO_x emissions.

Objectives:

decrease in SFC (specific fuel consumption)

By increasing:

overall pressure ratio (OPR) to 50:1

turbine entry temperature (TET) by + 100°C

the thrust to weight ratio (or power to weight ratio)

and raising the BPR to ~9

Key areas:

LPT

HPC

Gamma titanium aluminides

Gamma titanium aluminide based alloys have become an important contender for HT structural applications in the aircraft industry to replace current nickel-based superalloys for LPT blades.

The advantages achieved by the use of γ-TiAl intermetallics are

- **low density** (3.9-4.2 g/cm^3 as a function of their composition),
- high specific yield strength,
- high specific stiffness,
- substantial resistance to oxidation and good creep properties up to HT.

In particular, the lower density will contribute to **significant engine weight savings** and **reduced stresses** on rotating components such as LPT blades.

Although such materials appears very promising for the turbine engine industry, optimizing the performance improvements requires more advanced approaches to accurately predict fatigue life.

Therefore, there is a need to understand and address the **specific fatigue properties** of these materials to assure adequate reliability of these alloys in structural applications.

It is difficult to obtain a component produced with γ-TiAl intermetallics with exactly the composition and microstructure desired and in the typical aeroengines applications must have an extremely low oxygen content, preferably much lower than 1500 ppm.

Evolution of γ-TiAl

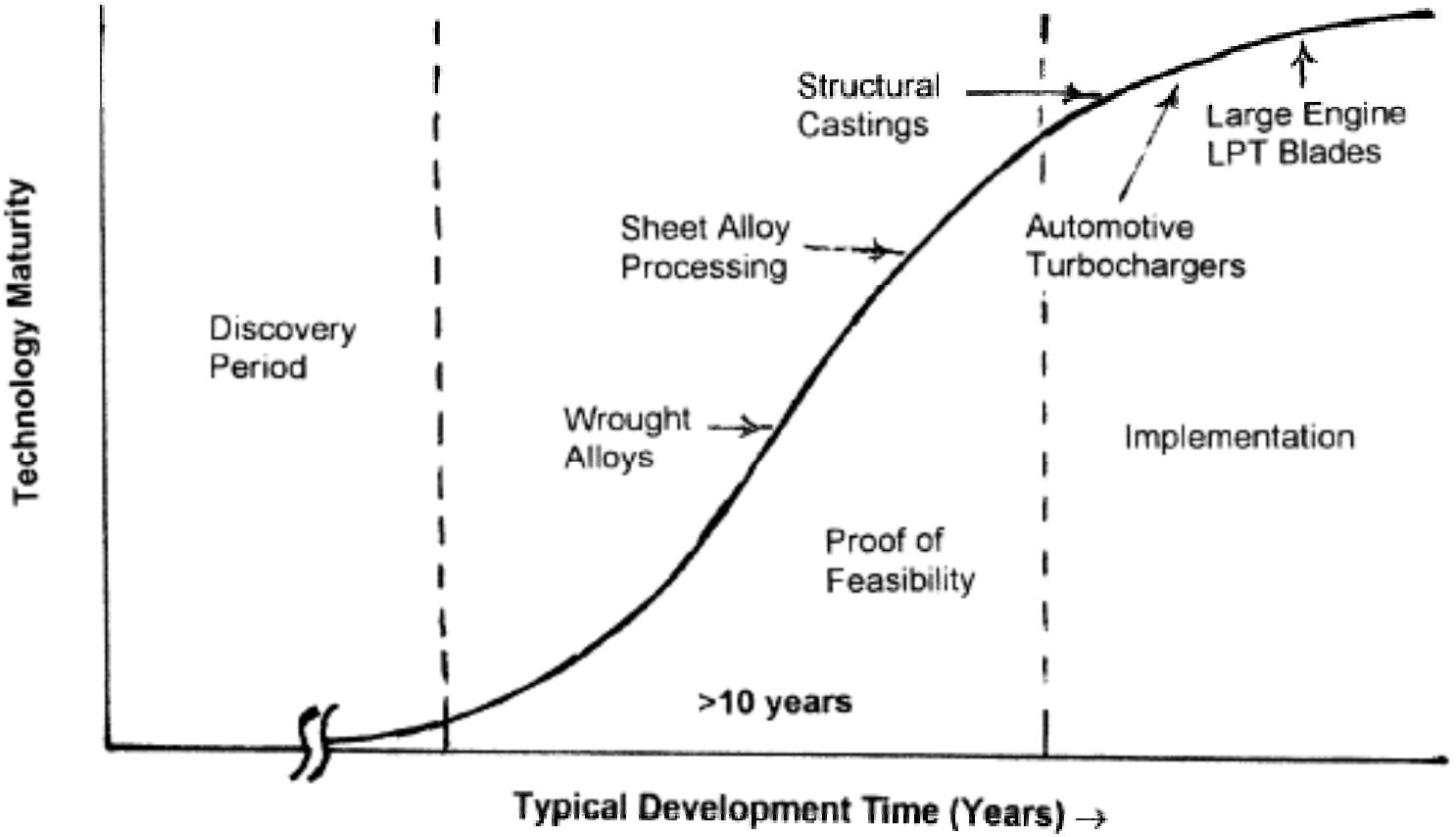

Evolution of gamma titanium aluminide technologies. General stages of maturity on undefined time scale, current stage of specific products relative to the development curve. [source: Loria, 2000]

Applications in LPT blading

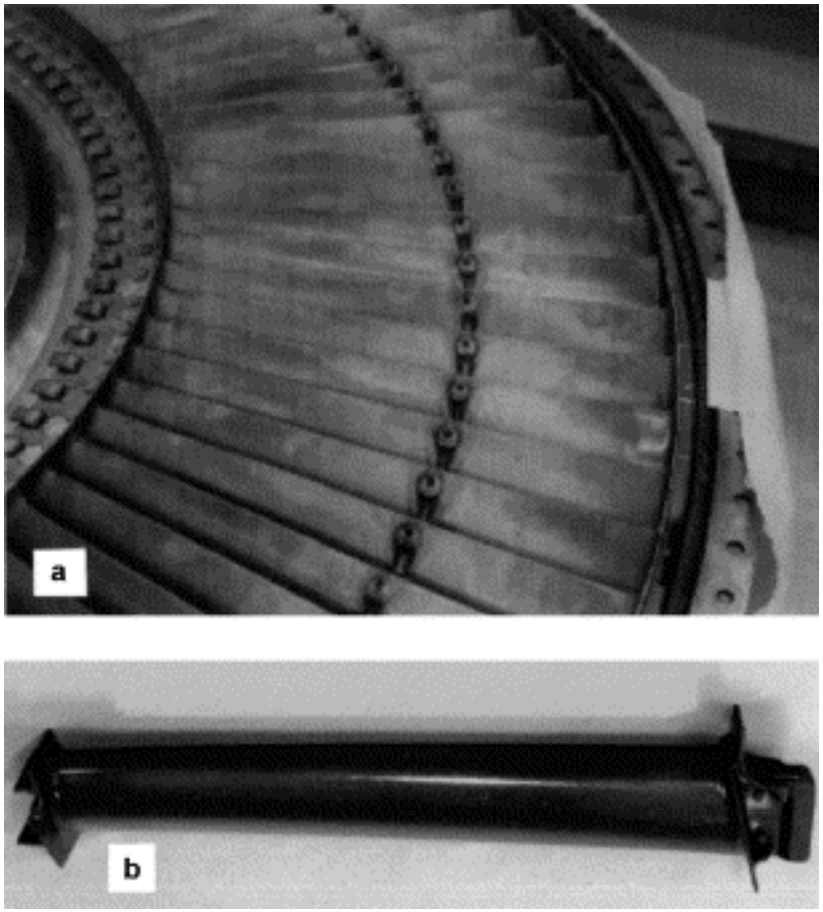

Complete Stage 5 rotor of cast γ-TiAl low pressure turbine blading for demonstration CF6-80C engine and an individual low-pressure turbine blade. [source: Loria, 2000]

Ten years on: where are we now?

From E. Loria, Intermetallics, 8(9-11), **2000**, pp. 1339-1345.

Even though the specific products and their properties have been demonstrated, there are still major issues to be resolved during this developmental period. […] The following factors that are considered most important to the subject products:

1. Alloy composition
   - …
   - Variations in composition and processing change many aspects of microstructure and a consequent variation in properties. […]
2. Desired process
   - Net-shape casting technology leads gamma alloy implementation
   - Certain aspect of casting process sets limits on properties.
   - Total production cost of cast blades has to be brought into balance with benefit.
3. Component definition
   - […]
   - **Variability in ductility and fracture toughness reduces confidence levels felt by component designers, in particular, the consequences of limited ductility at stress concentrators.**
   - Need to establish economy-of-scale and maximize process yield or reliability. A **maturing design practice** is needed.

Gamma Titanium Aluminide by EBM

- **Electron beam melting** (EBM) is a type of additive manufacturing for metal parts.
- It is often classified as a **rapid manufacturing** method.
- The technology manufactures parts by melting metal powder layer per layer with an electron beam in a **high vacuum**.
- The process of material production operates under **high vacuum** conditions, thereby reducing the risk of oxidation in the material of the final components.
- EBM technology for “layer by layer” productions offers several advantages with respect to other competing technologies and it is possible to operate at temperatures closer to the melting points of the intermetallic alloys.
- In the EBM process, components are produced without vaporization of the powders of the initial material and the powders are made of an intermetallic alloy based on titanium and aluminium with the same chemical composition as the final intermetallic with which the components are produced.
- The **Buy-to-Fly** ratio is how much material you need to purchase in order to manufacture the final flying part. The Buy-to-Fly ratio is as high as 15 or 20 for many flying components due to complex geometries, adding a lot of cost to the component.
- The **EBM process opens up an opportunity to produce light-weight titanium components with a Buy-to-Fly ratio close to 1**.

Fatigue tests at RT and HT

Material and specimen geometry

- The gamma titanium aluminide (γ-TiAl) Ti-48Al-2Cr-2Nb alloy studied in this work has been produced according to a patented process with EBM A2 machine manufactured and distributed by ARCAM AB (Sweden), which allows focused electron beam melting to be performed in high vacuum conditions.
- Material has been produced in the form of near net shape specimens.
- Final specimens geometry was realized by conventional machining with carefully selected cutting parameters for removing the machining allowance.
- Prior to RT fatigue testing, the surface of the specimens has been pre-oxidized, by furnace treatment in air for 20 hr at a temperature of 650°C

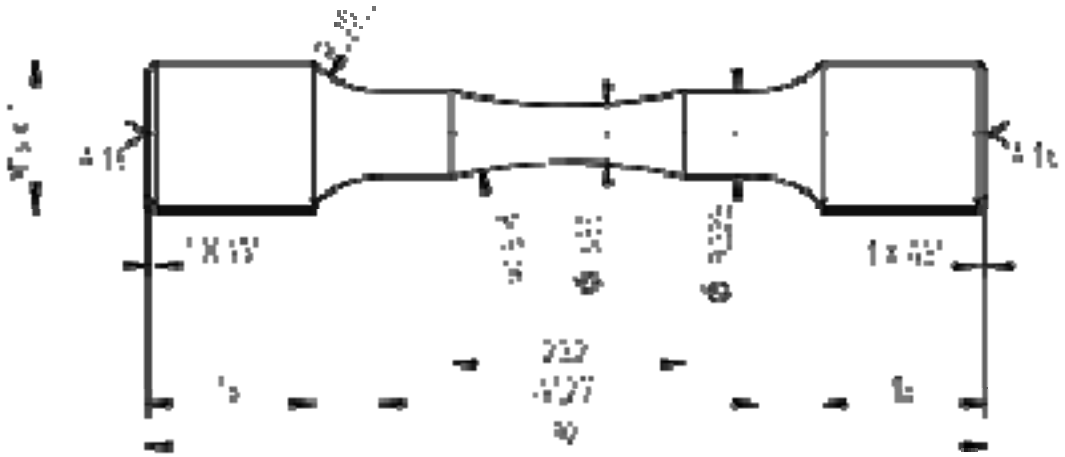

High temperature HCF test setup

Fatigue test method: plain specimens

To control the temperature during tests, 2 thermocouples are spot welded on every specimen (one gives feedback signal to the induction heater controller, one for cross checking with an independent acquisition system)

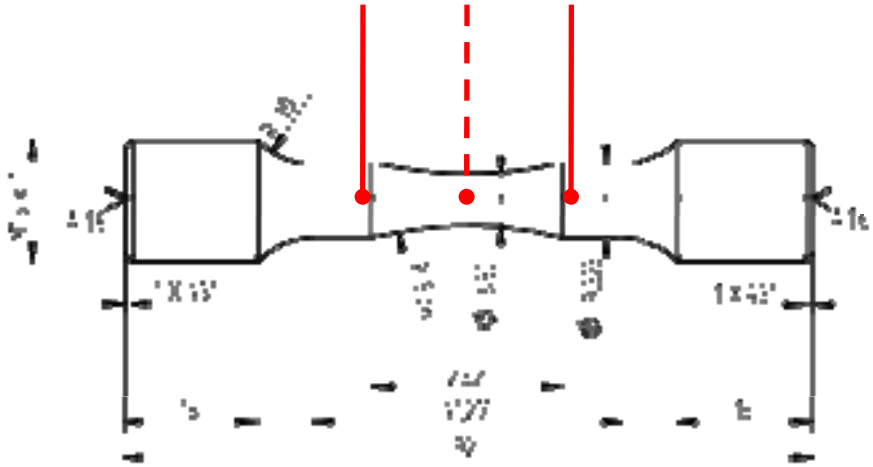

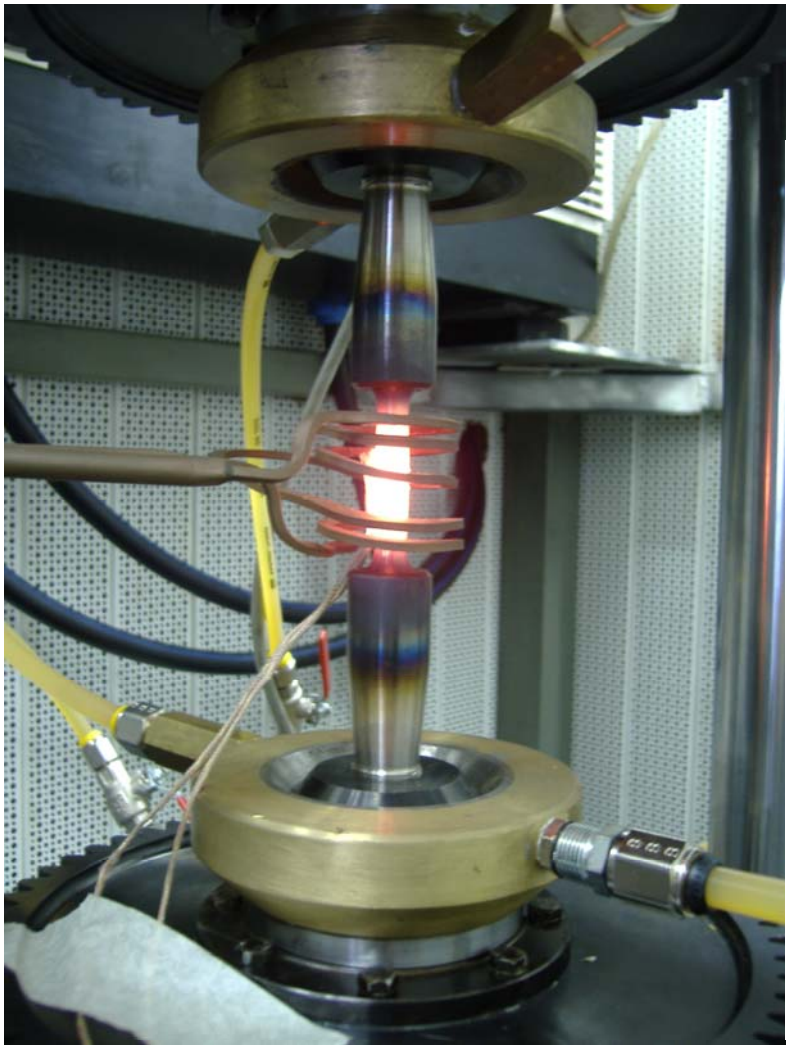

Fatigue test plan

Fatigue tests have been conducted by applying the staircase technique and the number of cycles of censored test (runout) has been fixed at 10^7 cycles.

Tests have been carried out with three different loading ratio:

1. $R=\sigma_{min}/\sigma_{max}=0$ (zero to tension);
2. $R=\sigma_{min}/\sigma_{max}=0.6$;
3. $R=\sigma_{min}/\sigma_{max}=-1$ (pure alternating stress).

The HT fatigue tests have been carried out in the following conditions:

1. R=0 at 704 °C (1300 °F);
2. R=0.6 at 704 °C (1300 °F);
3. R=0 at 760 °C (1400 °F).

RT HCF test results at R=0.6

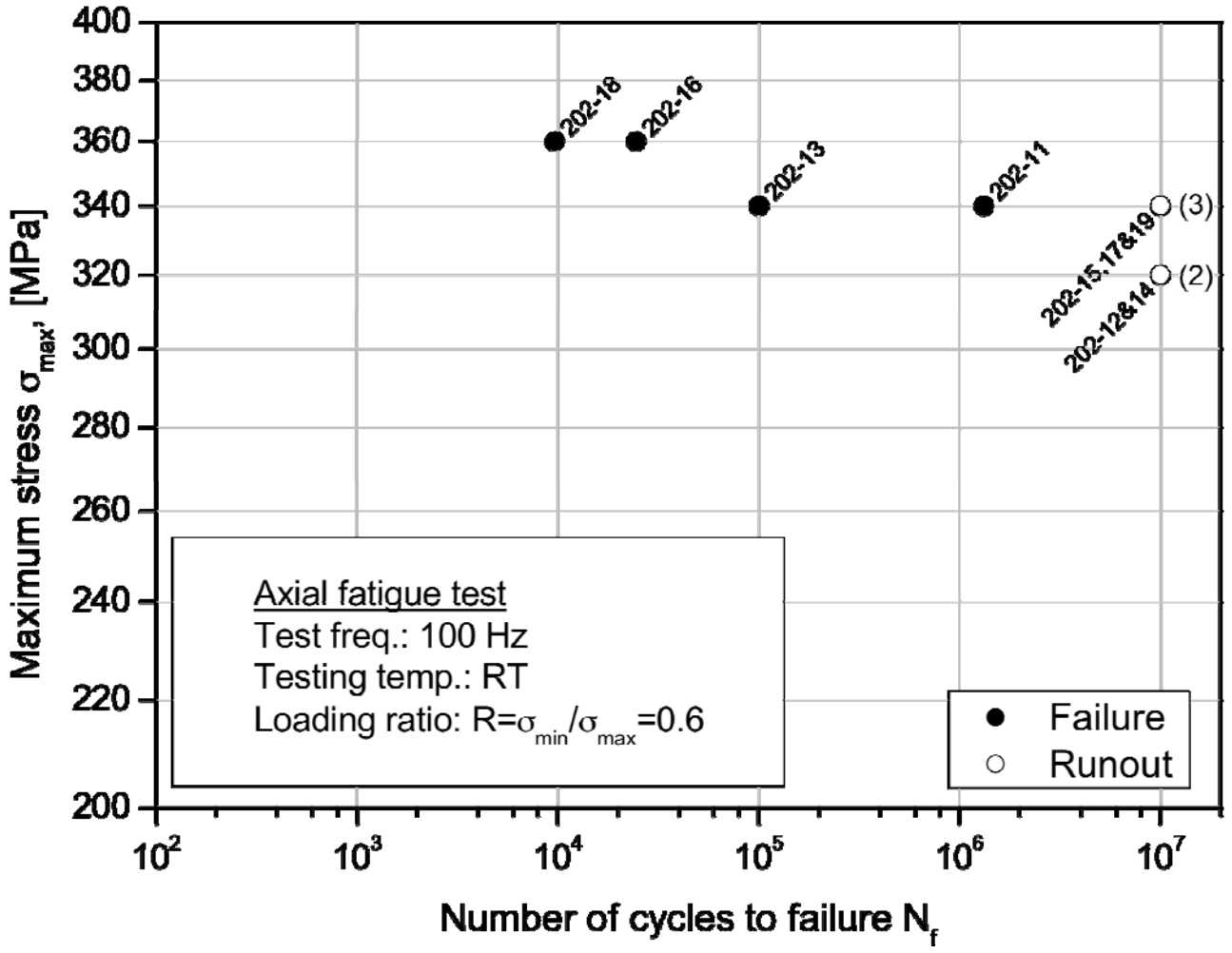

HT HCF test results at R=0.6

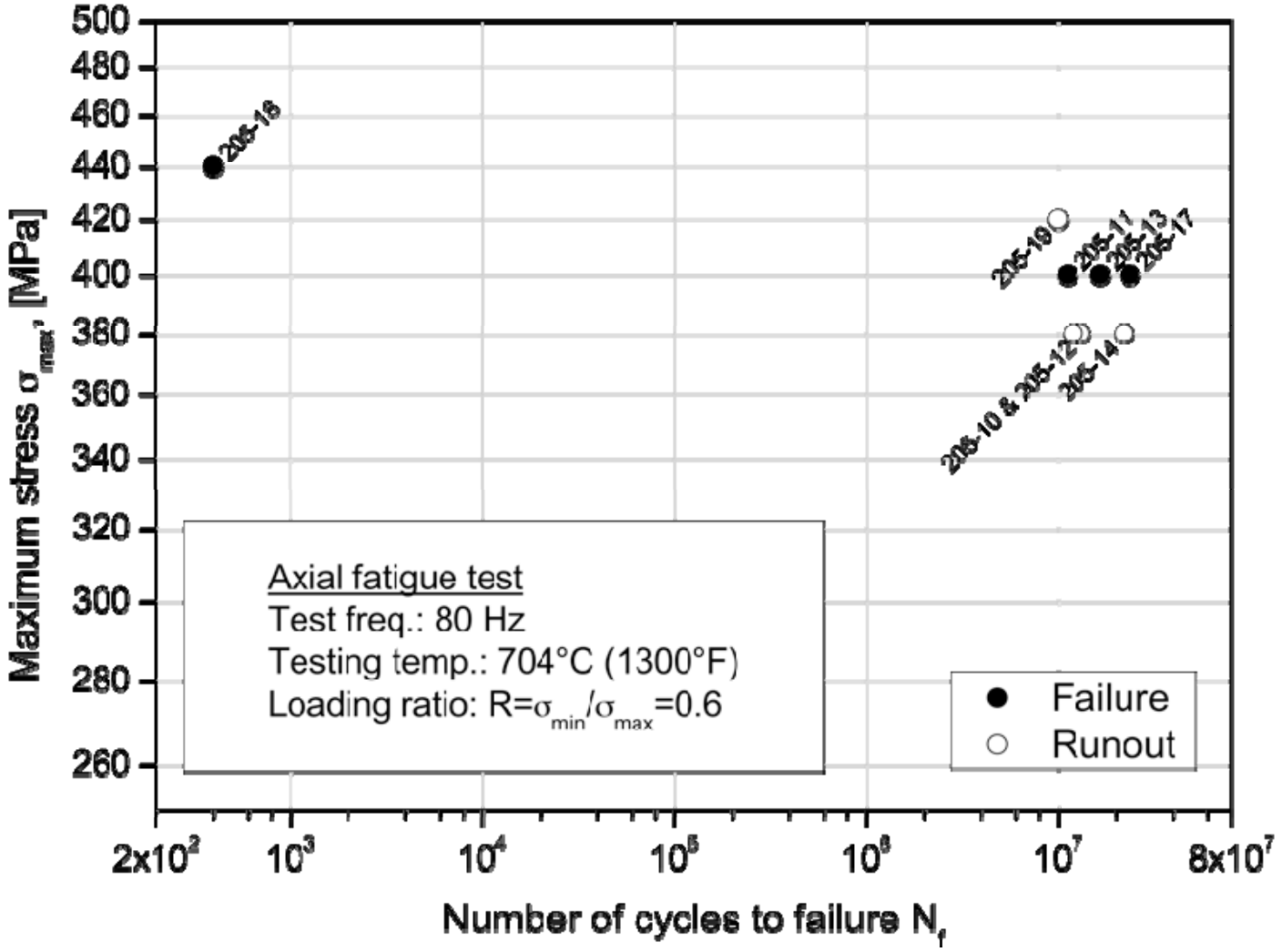

Haigh (modified Goodman diagram)

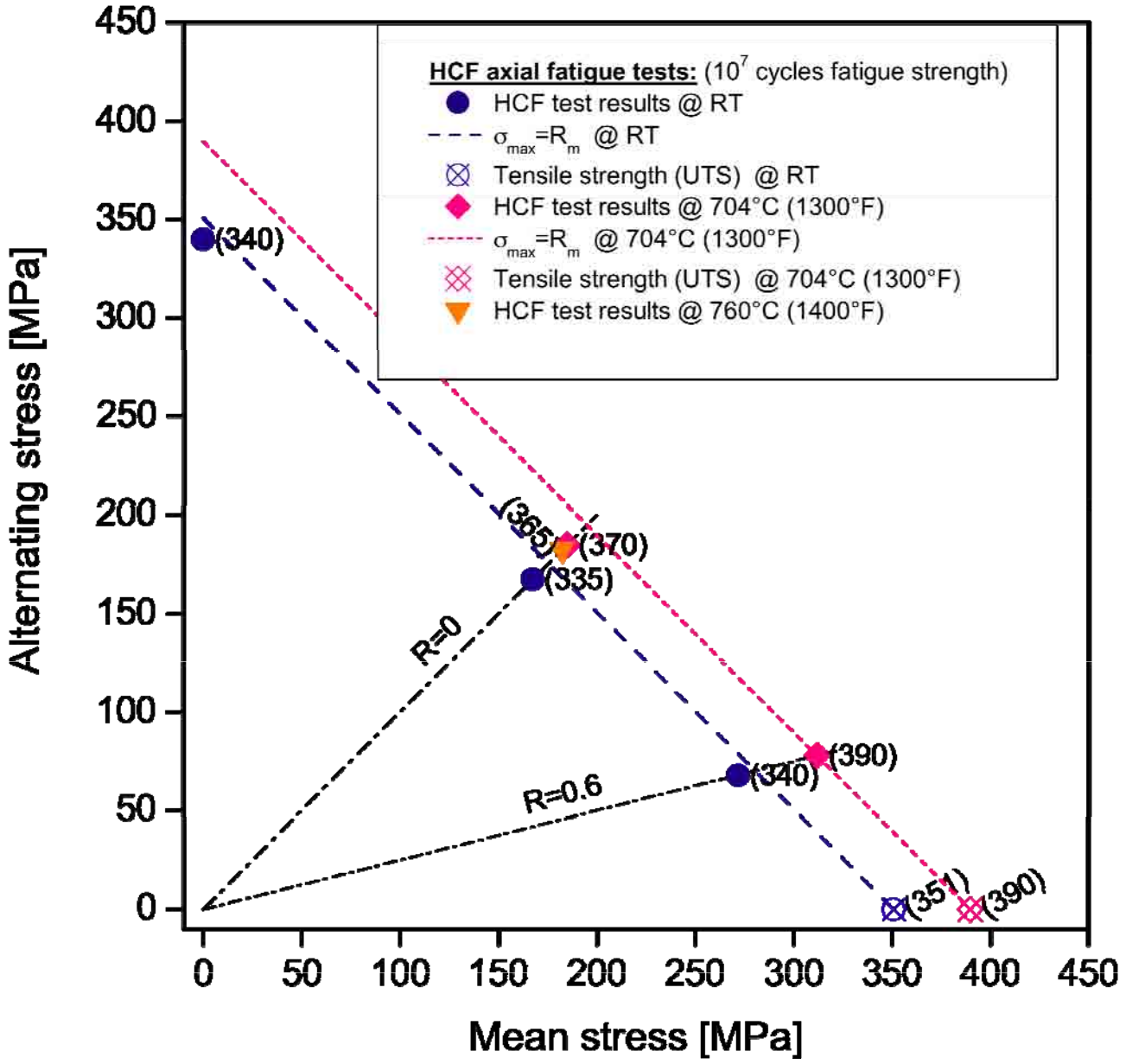

GE Aviation data

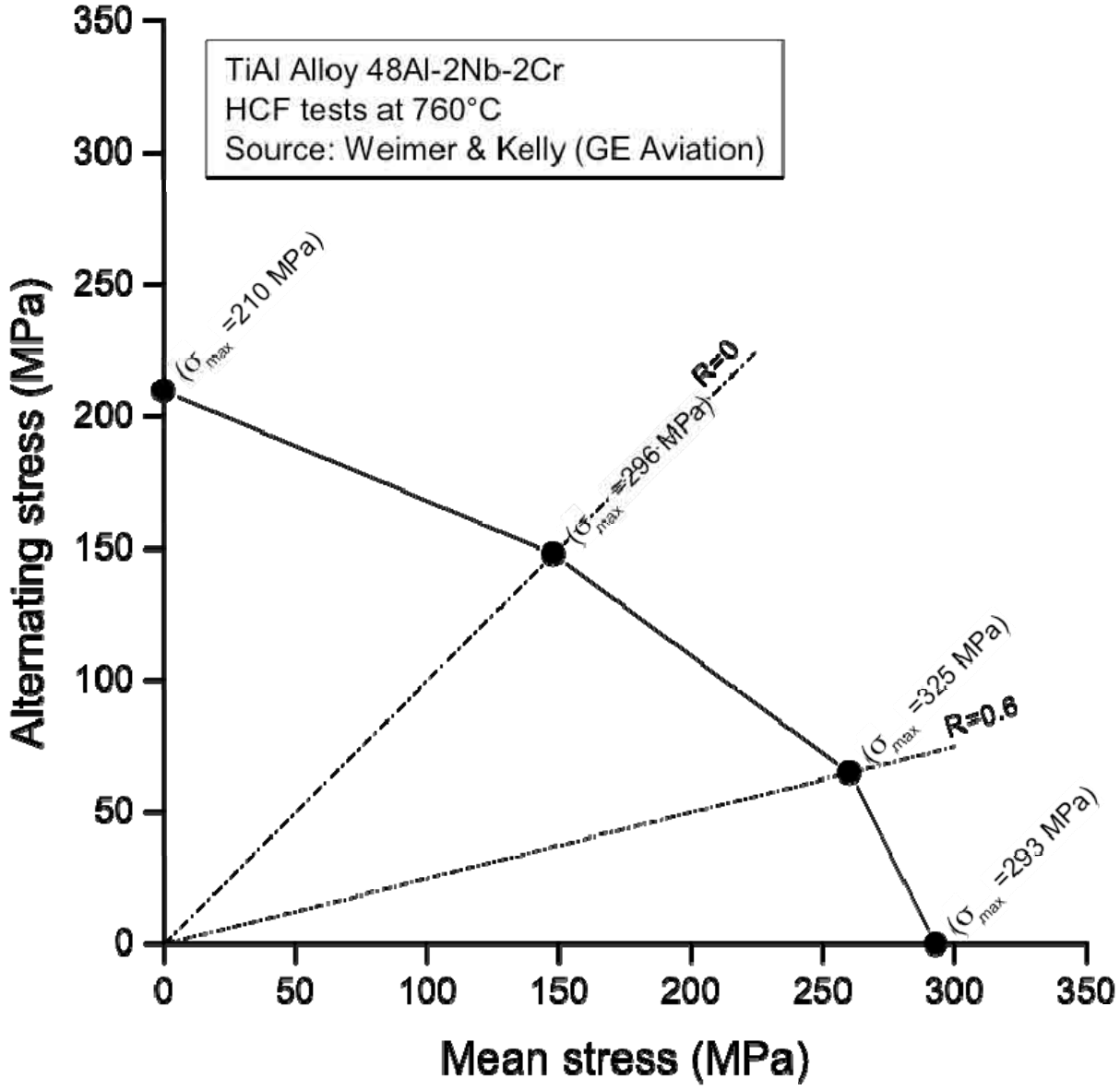

Fatigue crack growth tests at RT

FCG: specimen geometry

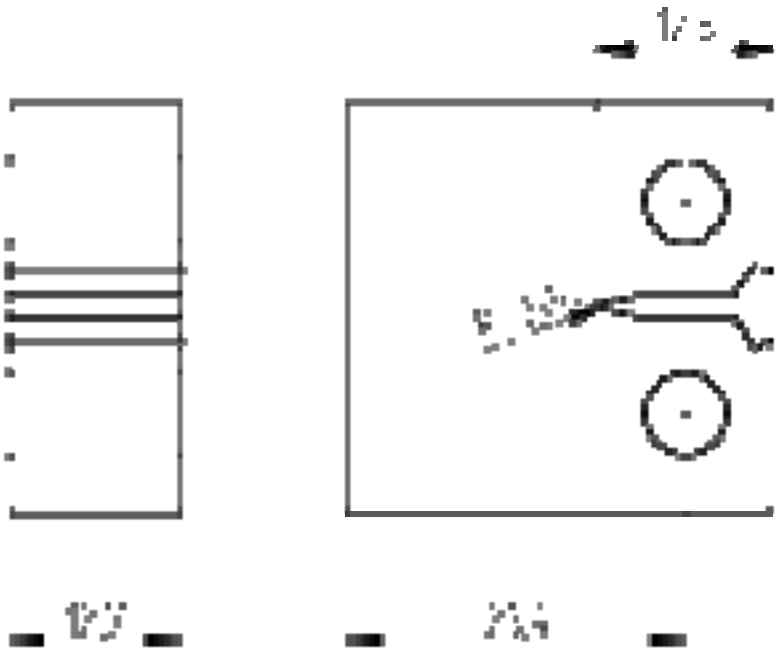

A set of 6 specimens suitable for crack propagation testing at room temperature have been produced with the geometry shown.

In the FCG specimens a starter notch has been produced by wire EDM with carefully selected cutting parameters, in order to avoid local modifications of the material microstructure.

Pre-cracking procedure – CT 1

Compression-Compression Pre-Cracking

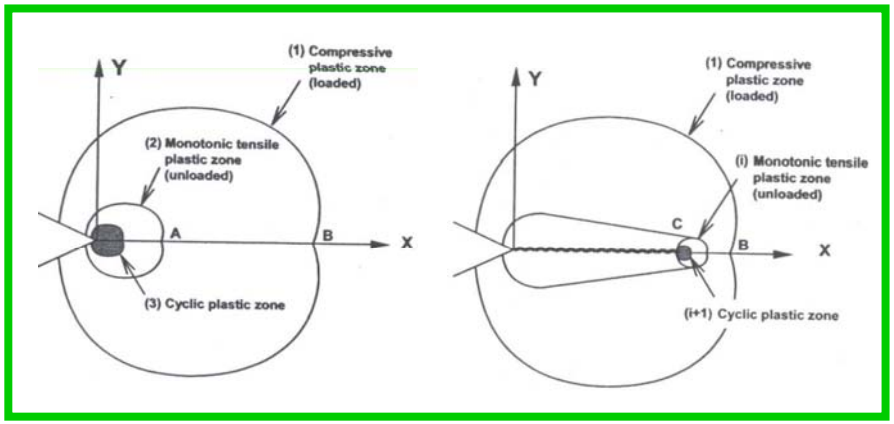

Specimen	Fmean [kN]	Range [kN]	ΔK [MPa√m]	Freq. [Hz]	n° cycles	Data	p.c.A [μm]	p.c.B [μm]	Notes	a_o [mm]
128-1	-1,05	0,85 x 2	4,2	73	4421500	15/09/2009	/	/	**No pre-crack**	6,43
	-1,22	0,99 x 2	4,9	74	1935300	16/09/2009	/	/	**No pre-crack**	6,43
	-1,38	1,12 x 2	5,5	75	3930300	16/09/2009	/	/	**No pre-crack**	6,43

We need a different way to produce a pre-crack!

Single Edge V-notch Beam (SENVB) method (for ceramic materials)

SENVB method

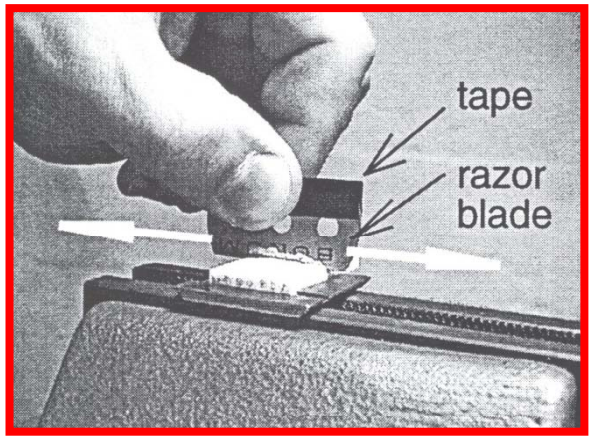

Very shallow notch

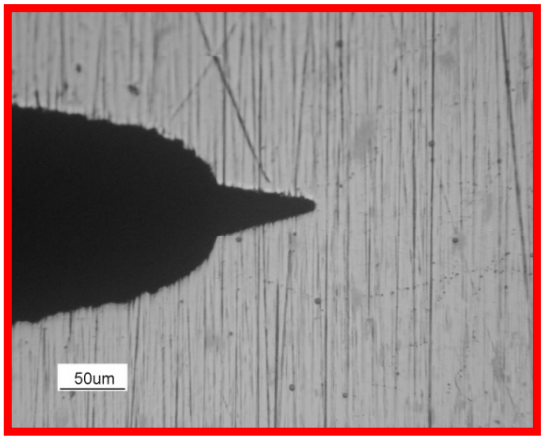

The crack growth test has been carried out with the specimen n°1 with the new shallow notch.

Several steps at increasing ΔK, without any evidence of crack growth until a final step at ΔK=10 MPa√m with **failure upon loading** (monotonic loading)

New pre-cracking procedure

SENVB method

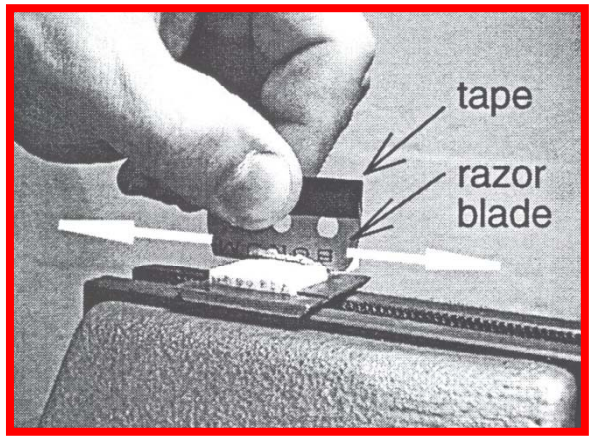

Very shallow notch

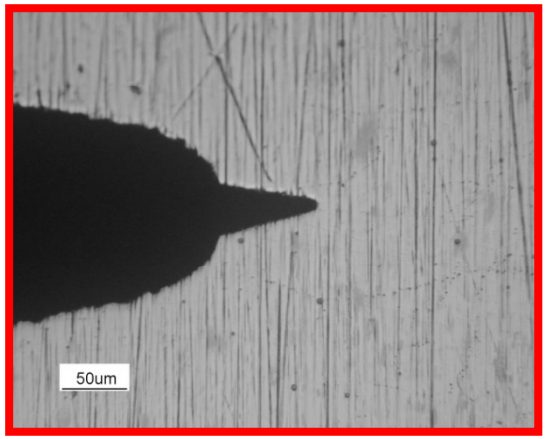

Compression-Compression Pre-Cracking

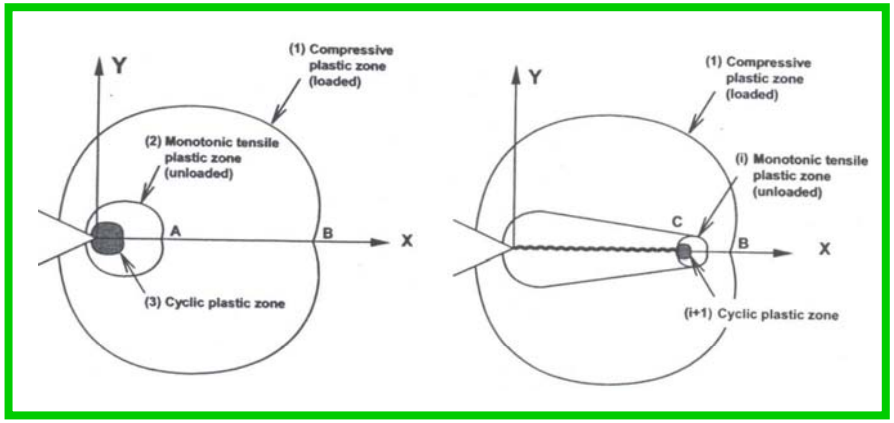

Minimal load history effects

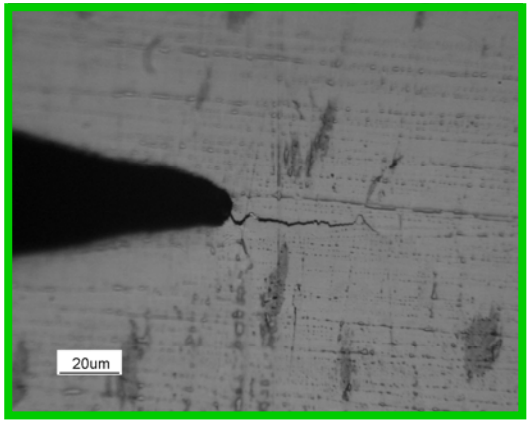

Notch radius influence

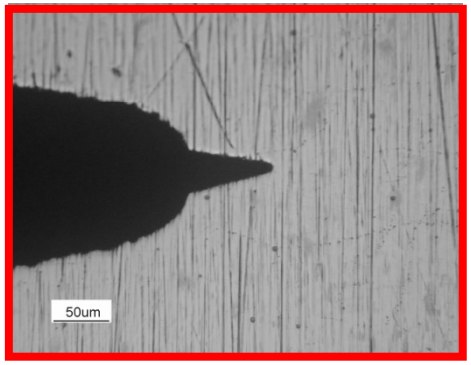

Linear-elastic material

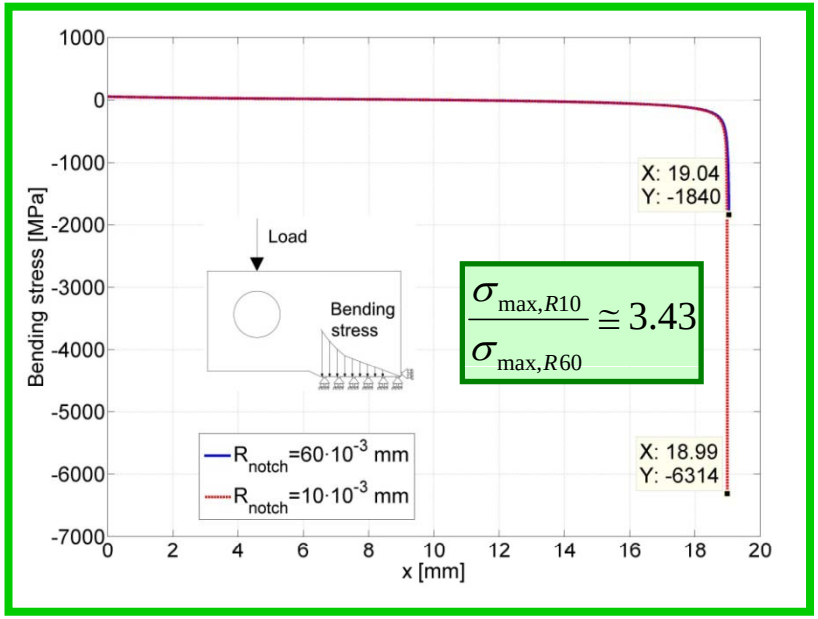

Elastic-plastic material

2D FE analysis

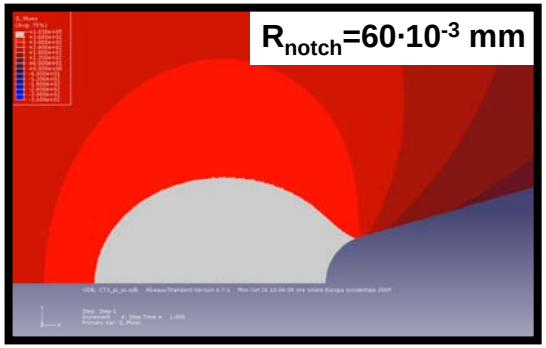

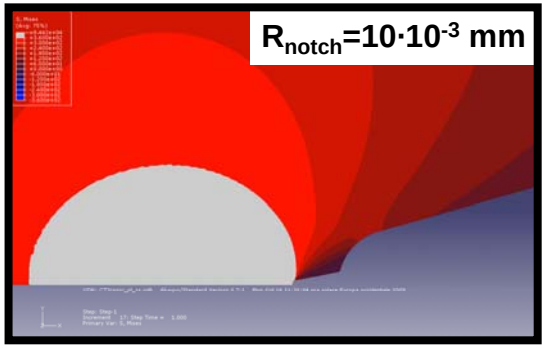

A smaller notch radius doesn't change the extension of the monotonic plastic region

SEVNB method + Compression pre-cracking – CT 3

Original notch – side A

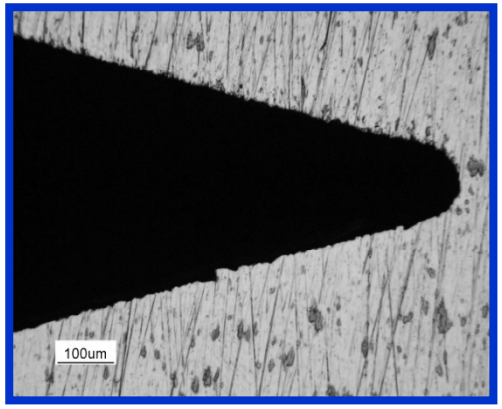

SEVNB method – side A

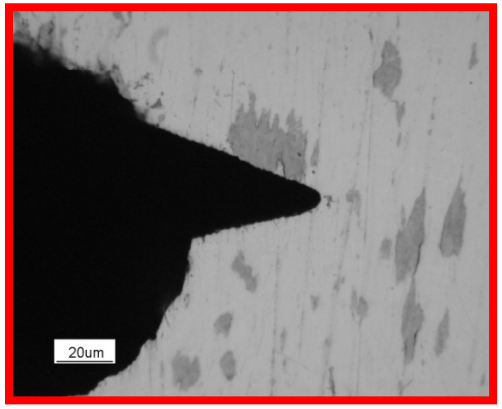

Δa_{SEVNB} = 48 µm; r_{notch} = 4 µm

Compression pre-cracking – side A

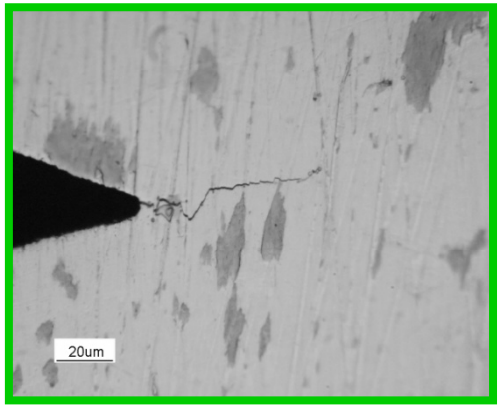

$\Delta a_{pre\text{-}crack}$ = 65 µm

Original notch – side B

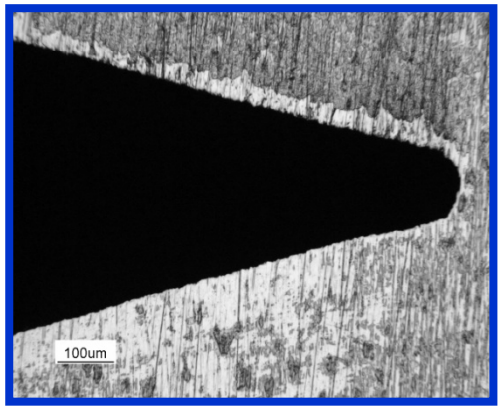

SEVNB method – side B

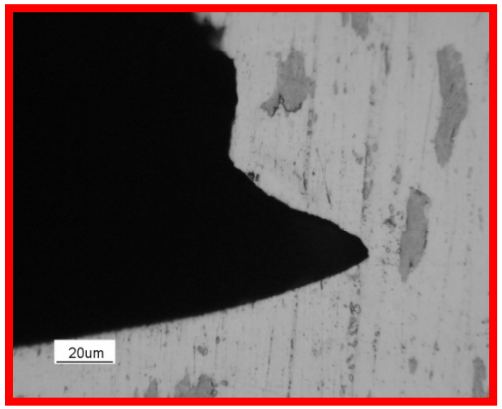

Δa_{SEVNB} = 47 µm; r_{notch} = 4 µm

Compression pre-cracking – side B

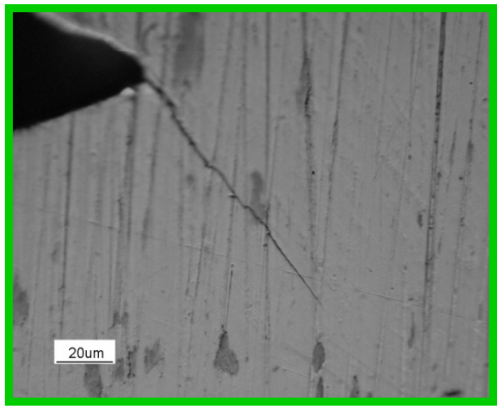

$\Delta a_{pre\text{-}crack}$ = 65 µm

Test machine for FCG tests

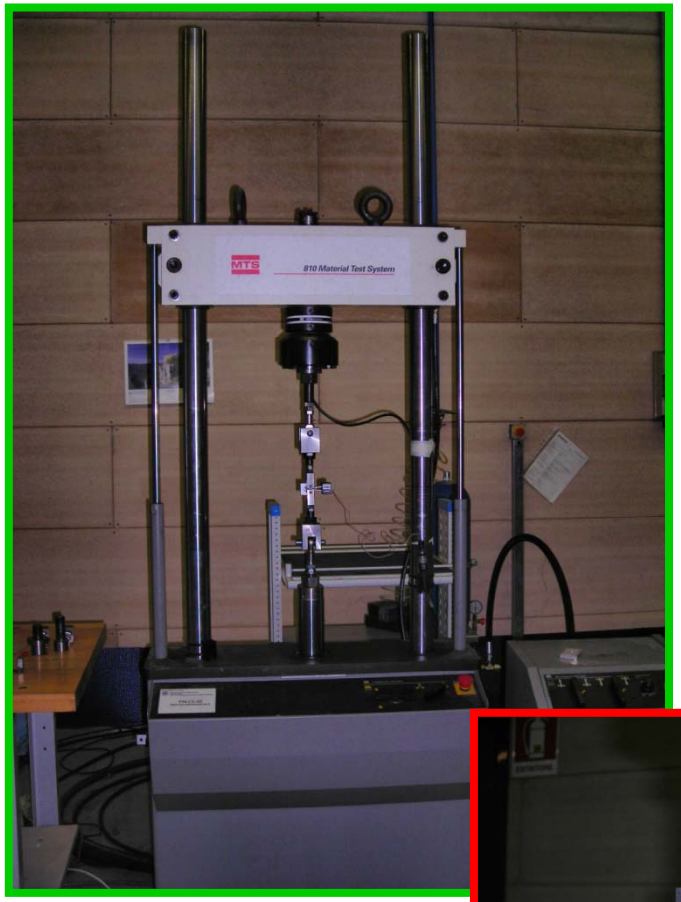

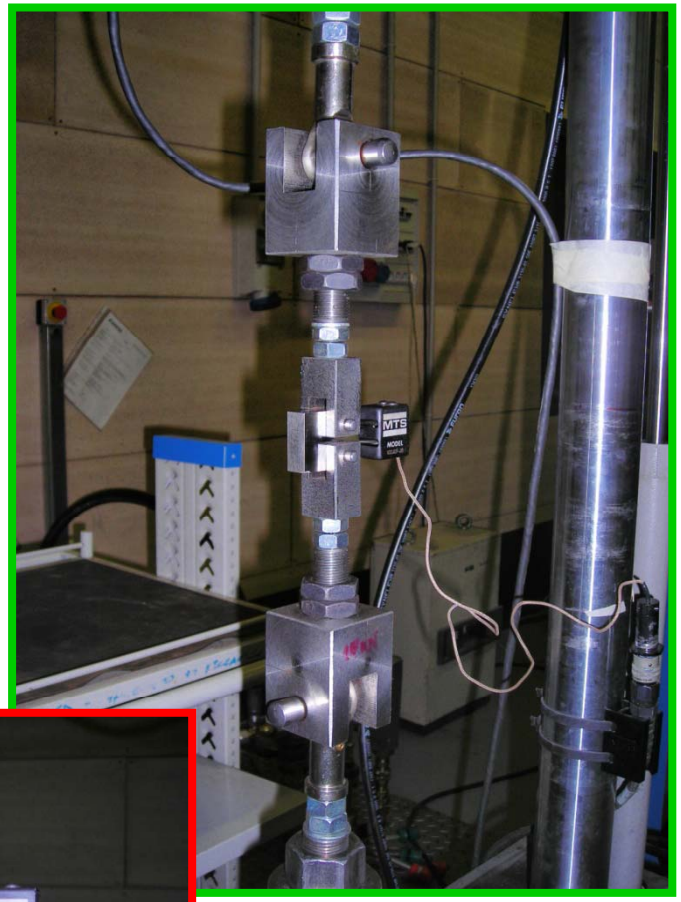

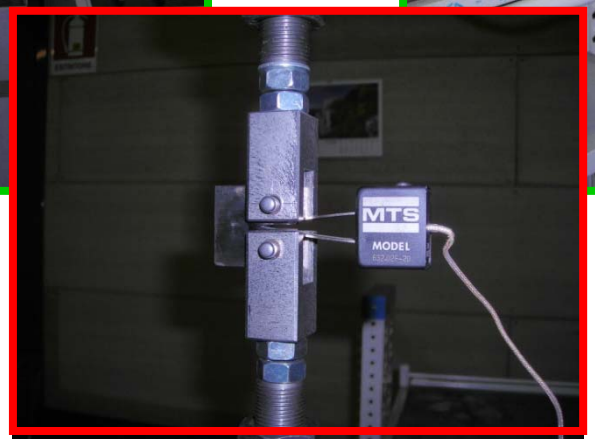

Crack growth test - CT 3

In the initial part of the crack growth test the load increment corresponds at a maximum amount of ΔK = 0.5 MPa √m. The images show the cracks after the load increments reported. In this ΔK range the crack seems to be under the threshold value and the crack length increments showed for ΔK = 5.0 and 5.6 MPa √m has been determined by residual stresses due to the pre-cracking procedure. The crack starts its growth at about **ΔK = 6 MPa √m**.

Δn = 2470714, ΔK = 5.0 MPa √m
Δa = 0.074 mm

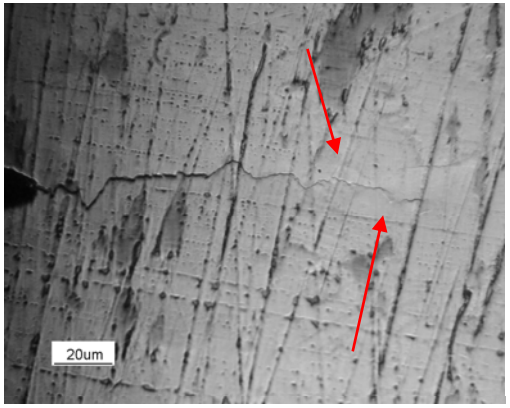

Δn = 676278, ΔK = 5.6 MPa √m
Δa = 0.096 mm

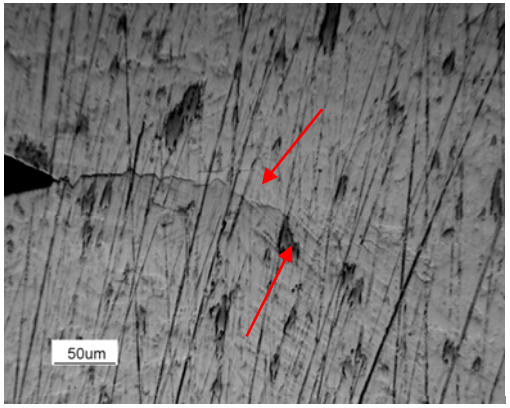

Side A

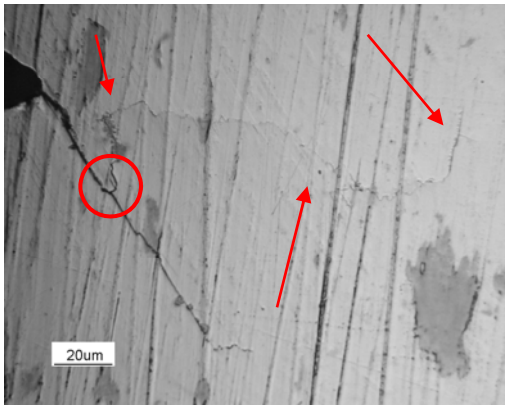

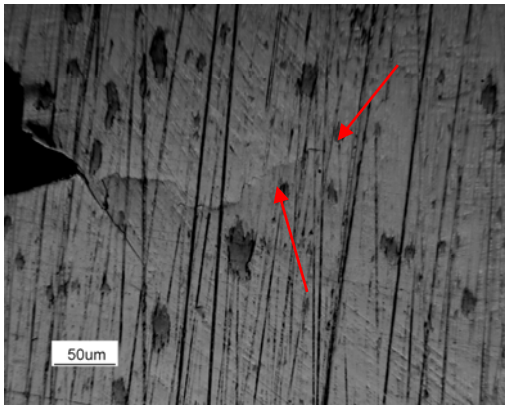

Side B

Crack growth test – CT 3 – R=0.05

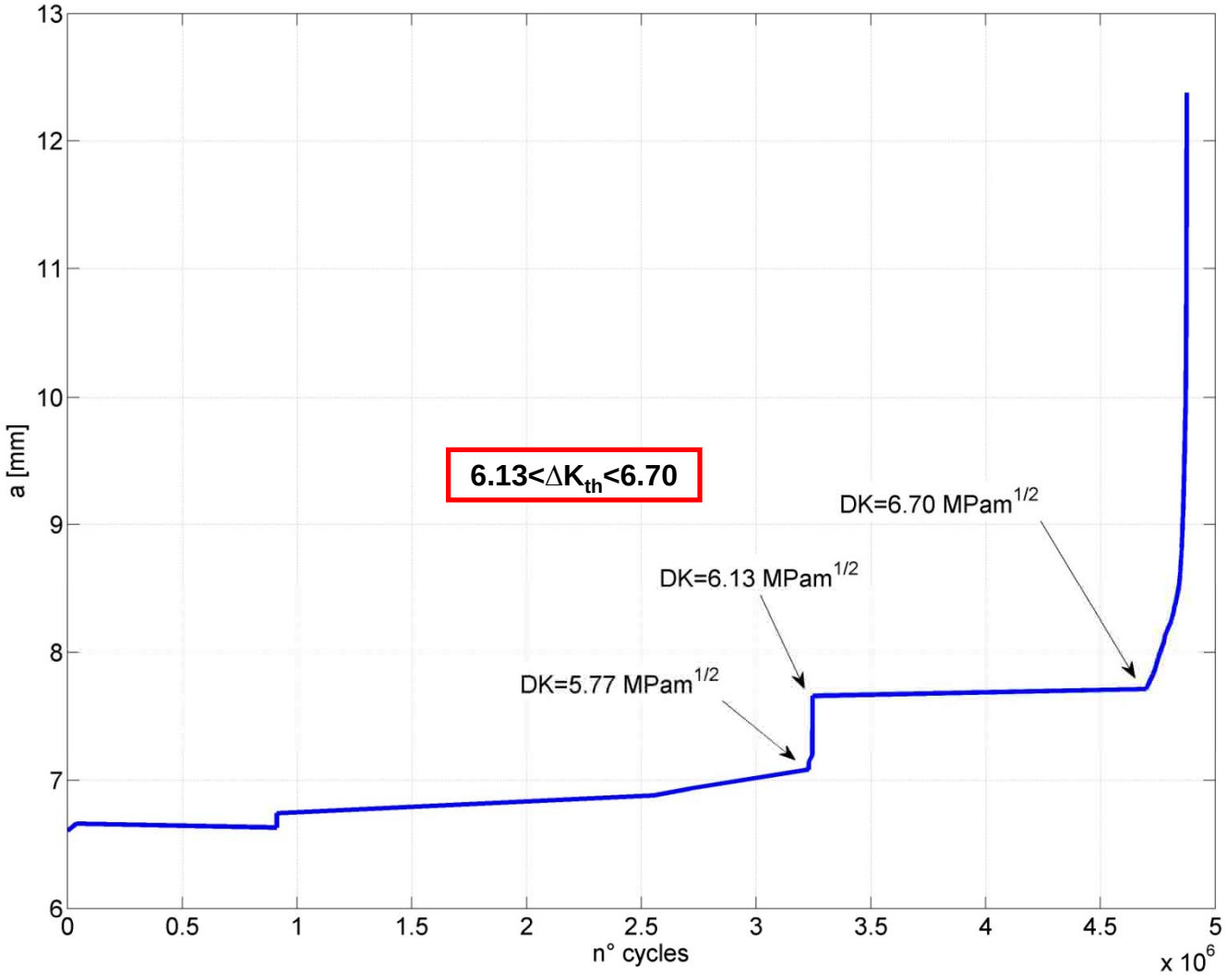

Crack growth test – CT 6 – R=0.05

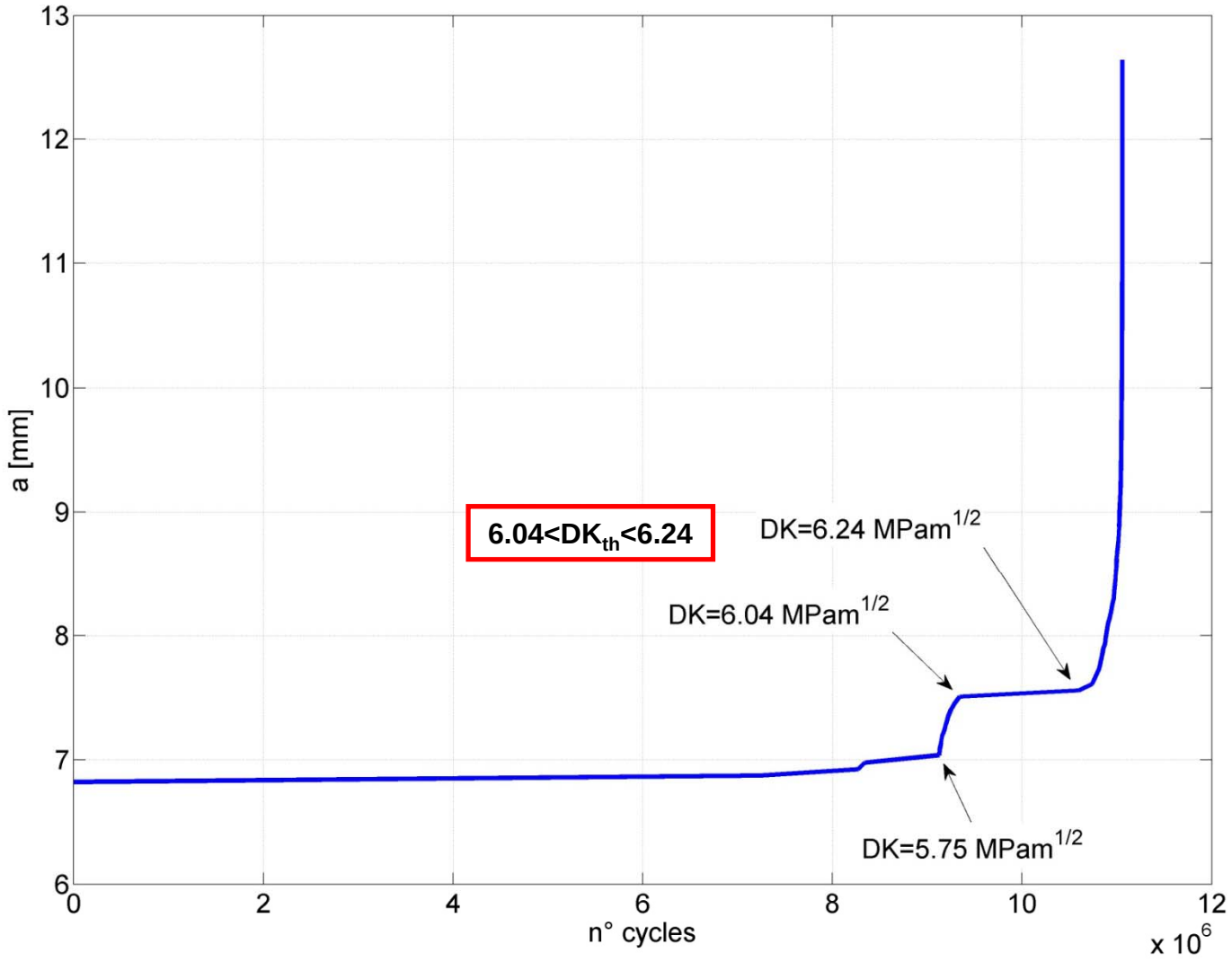

Crack growth test – CT 4 – R=0.6

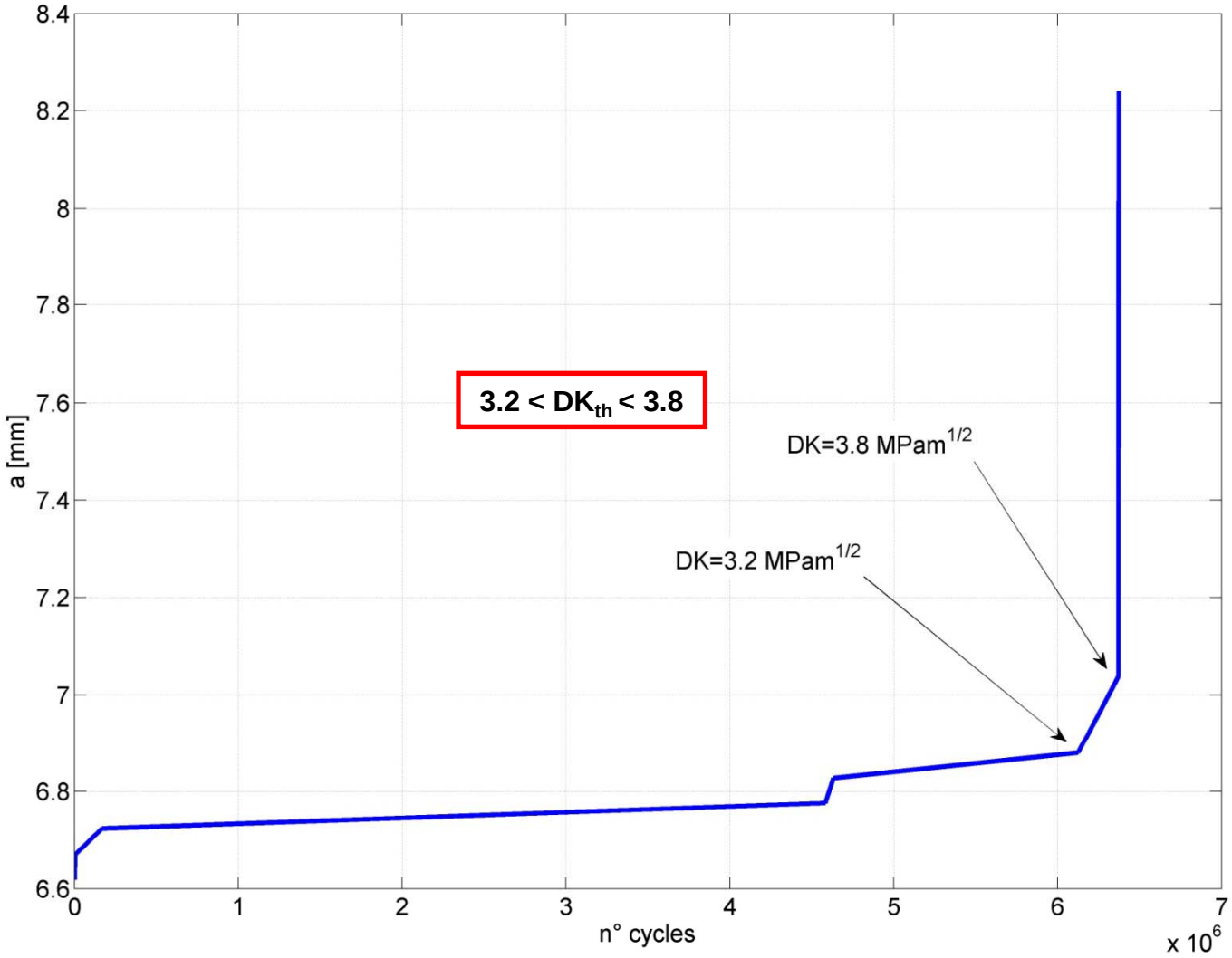

Crack growth test – CT 2 – R=0.6

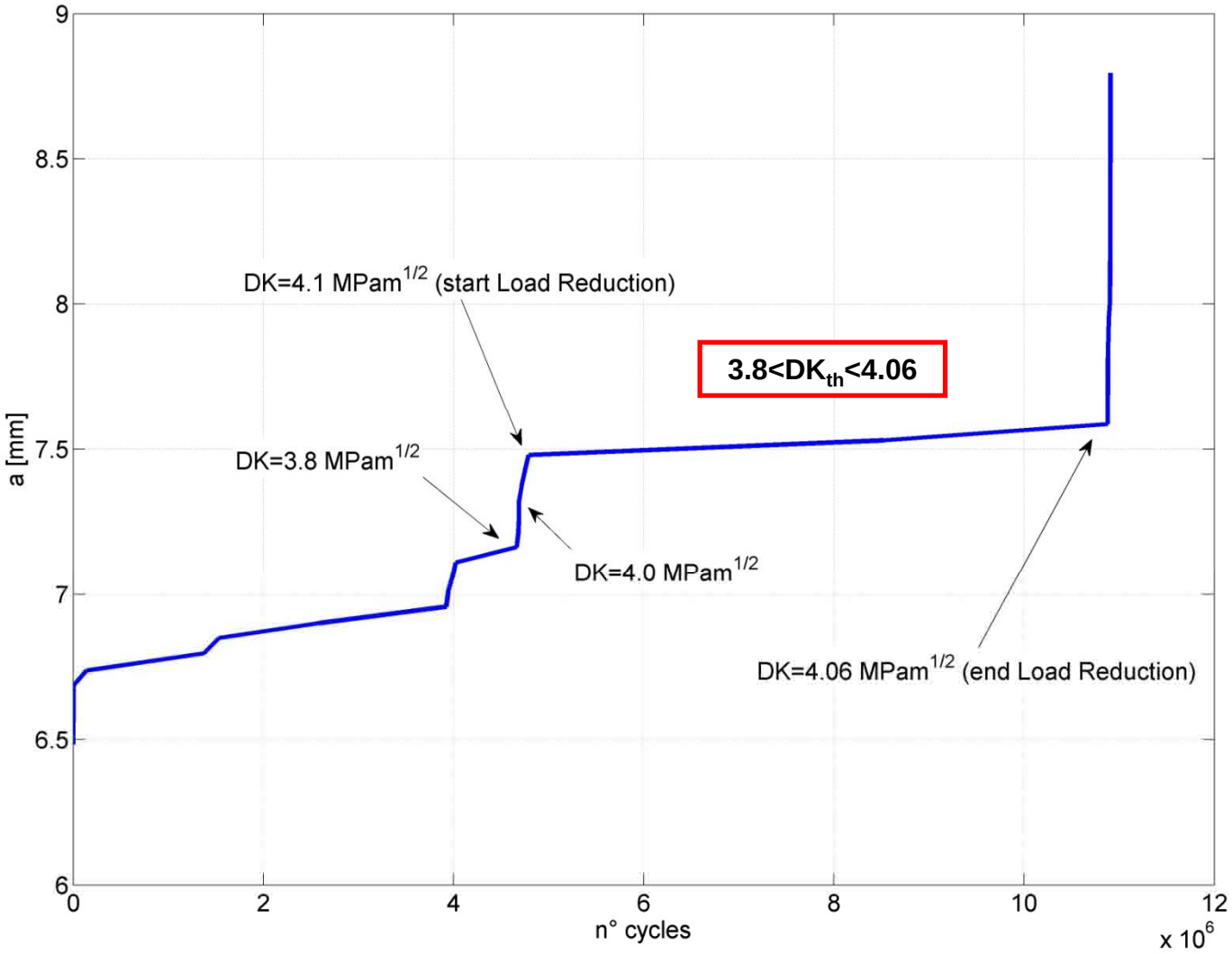

Crack growth test – da/dN vs ΔK

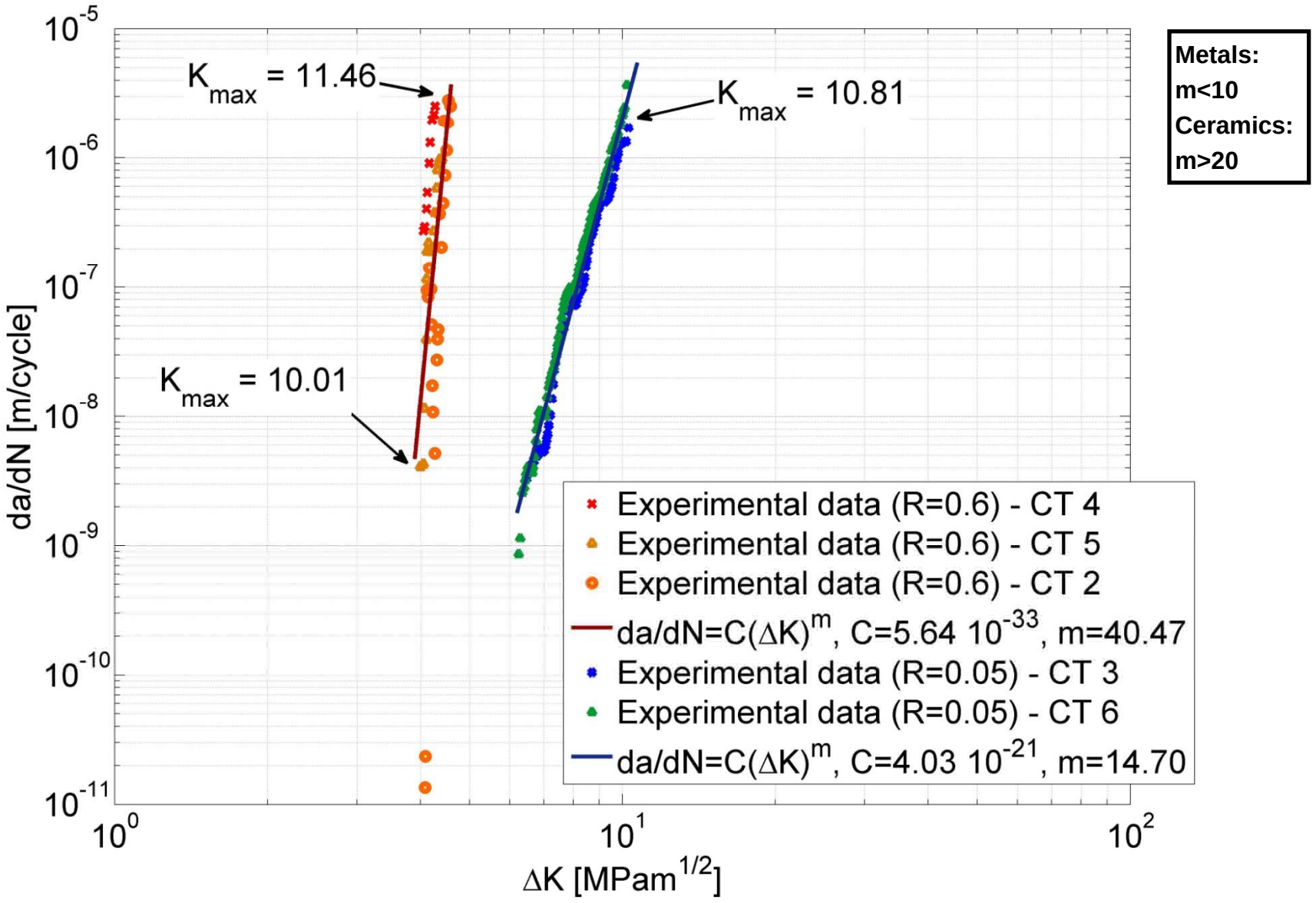

Crack growth test – Crack closure

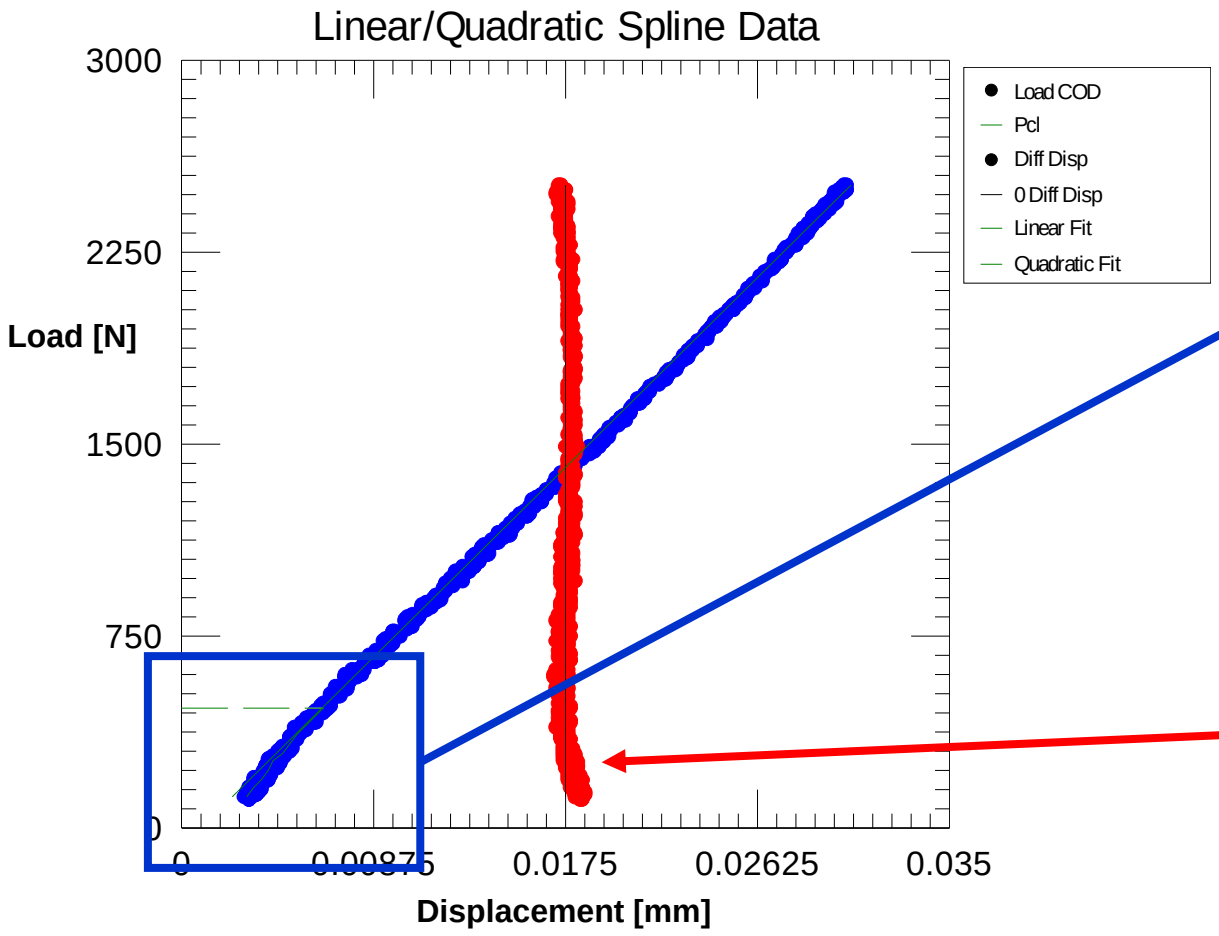

Cycle: 4737642

Diff. Displ. Multiplier: 1.0

Deviation of this points from the linear relation between Displacement and Load denotes the presence of ***crack closure***.

In order to evaluate the effect of the closure in the effective applied ΔK it has been analyzed the difference in the Displacement direction between the experimental points and the linear regression. In this way it is possible to calculate the load for which the crack closes before the achievement of the minimum load.

Crack growth test – Results

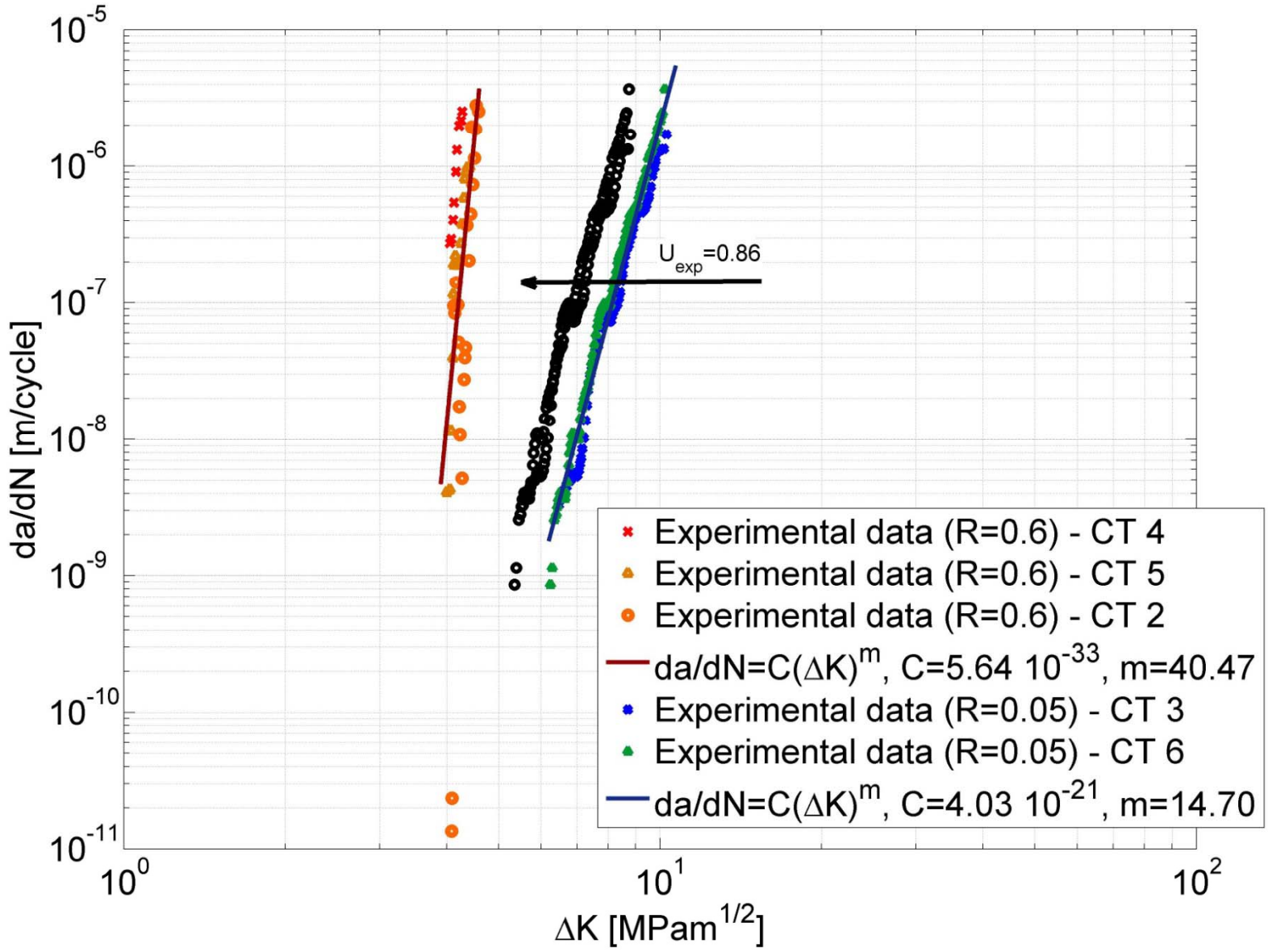

Crack growth test – da/dN vs K_{max}

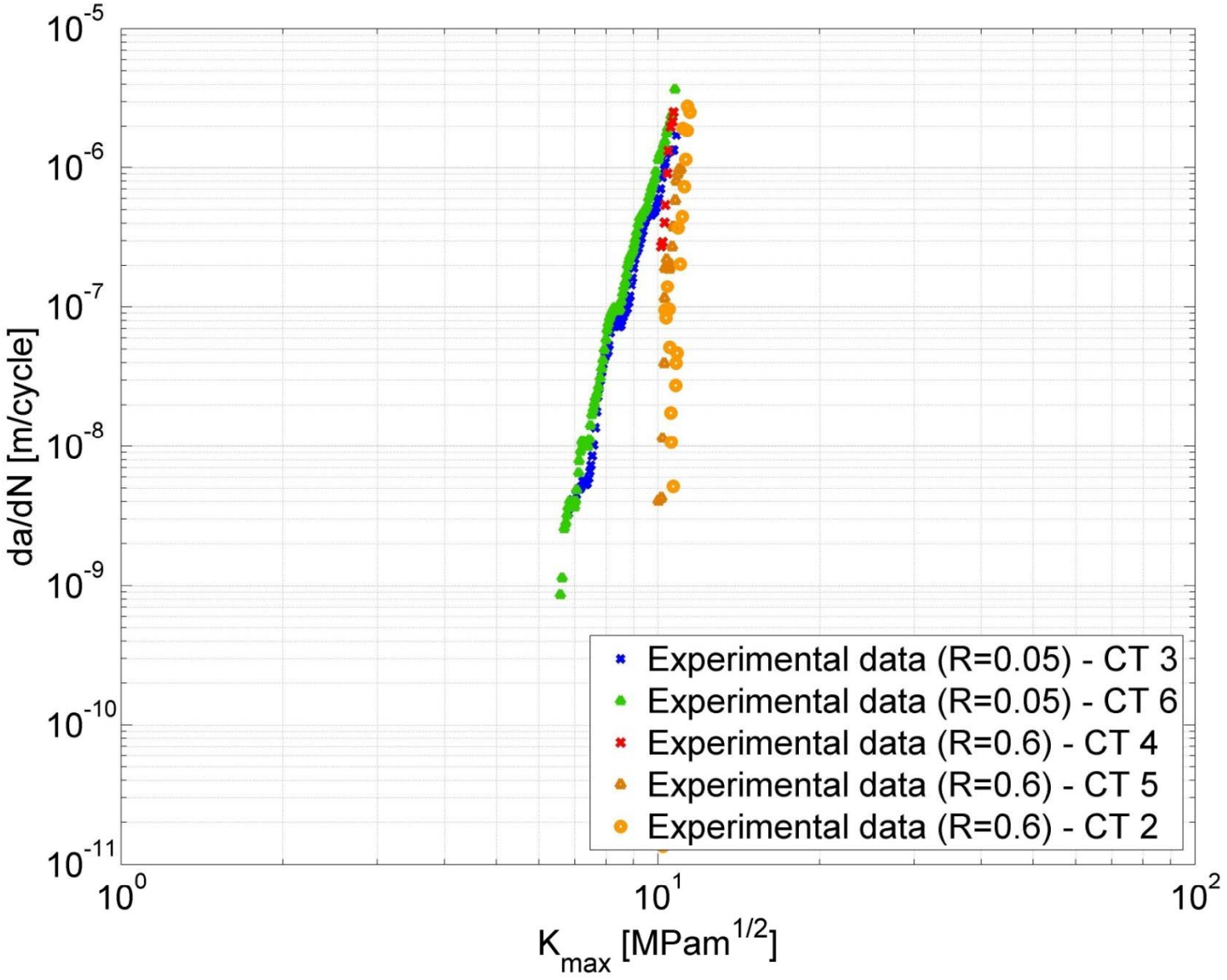

Analysis of fracture surfaces

SEM analysis: RT tests at R=0

Specimen S/N: **202-4**

Applied stress range: 340 MPa

Loading ratio : R=0

Maximum stress: 340 MPa

Minimum stress: 0 MPa

Number of cycles to failure: 3.2 10^6 cycles

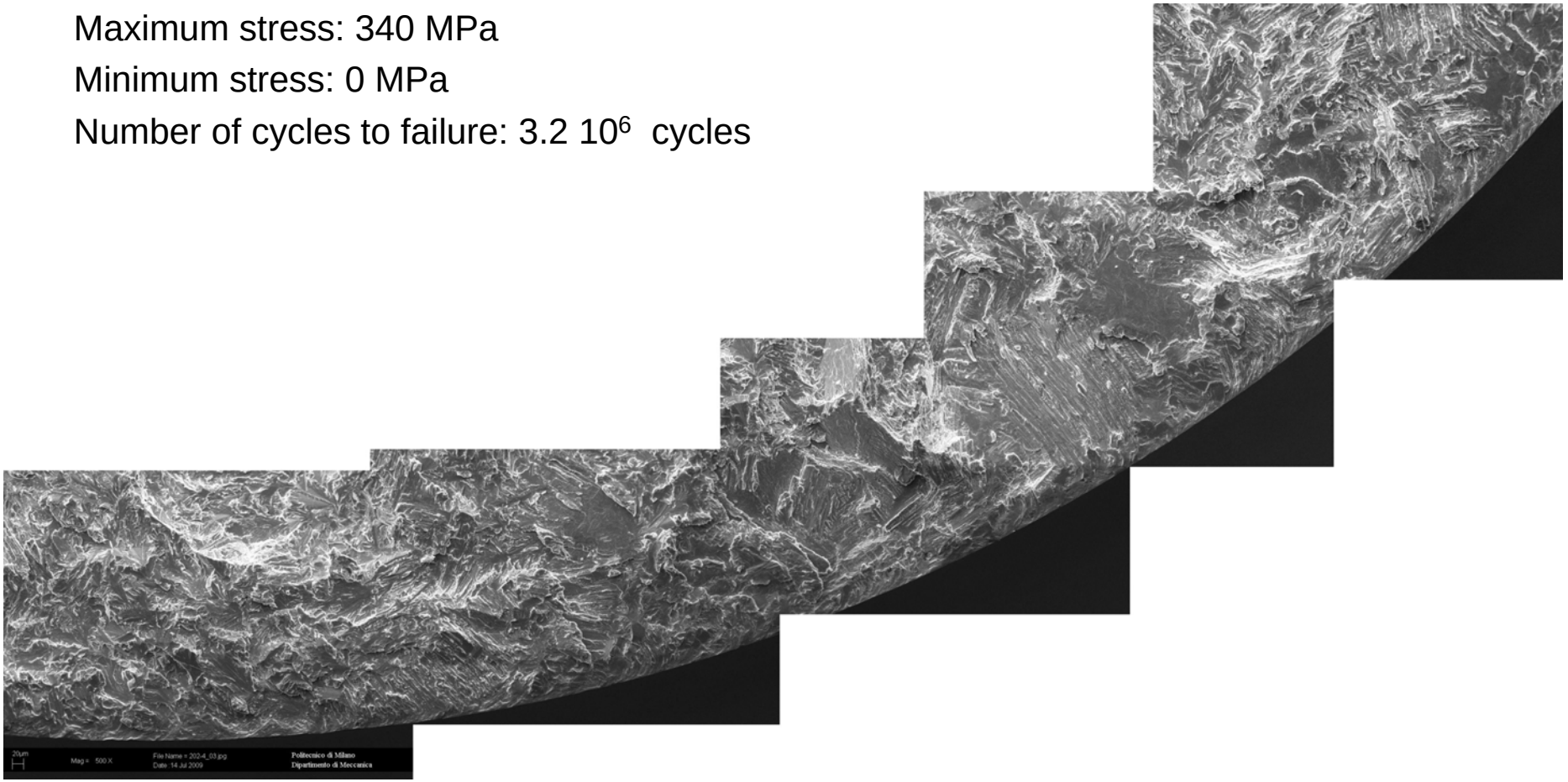

SEM analysis: RT tests at R=-1

Specimen S/N: **202-23**

Applied stress range: 680 MPa

Loading ratio : R=-1

Maximum stress: 340 MPa

Minimum stress: -340 MPa

Number of cycles to failure: 9.6 10^6 cycles

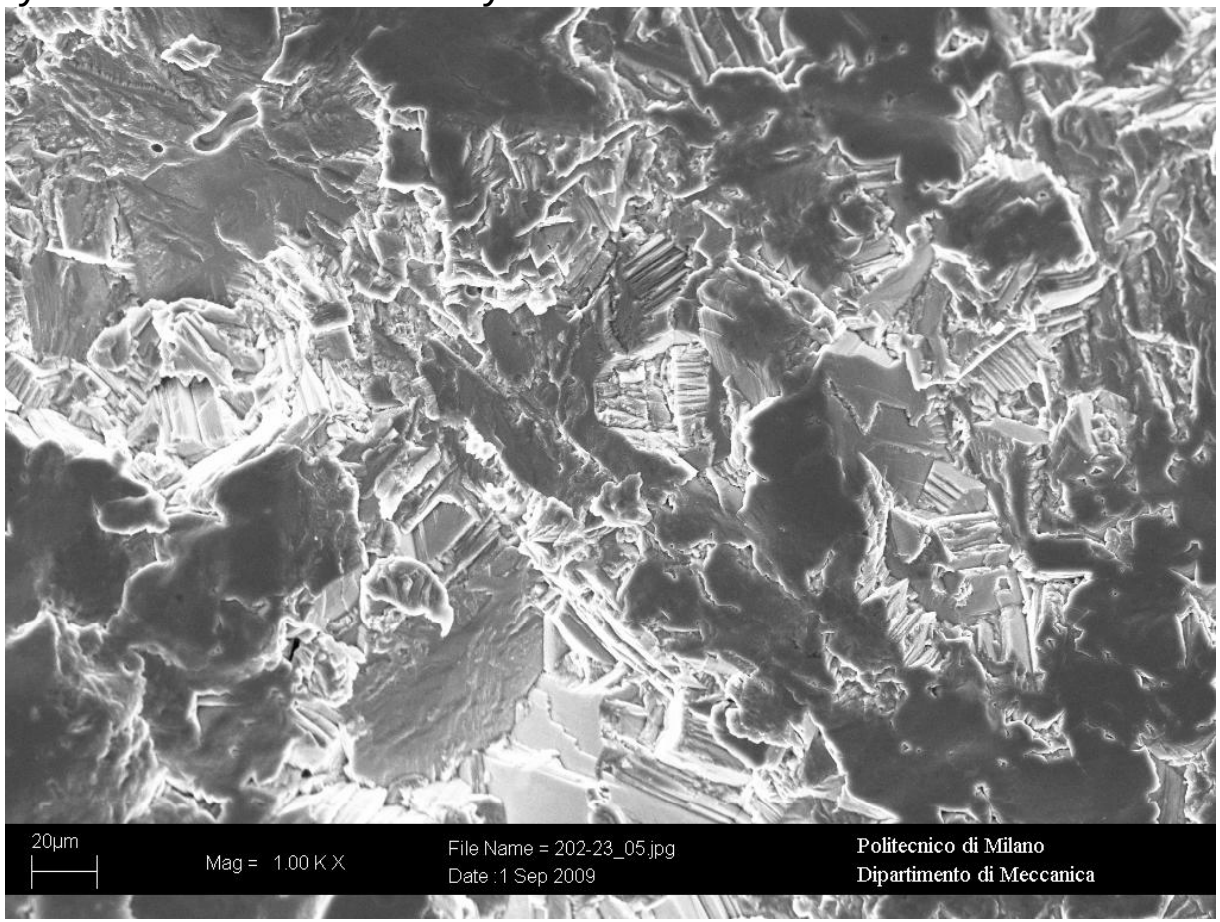

SEM analysis: tests at R=0.6 (704°C)

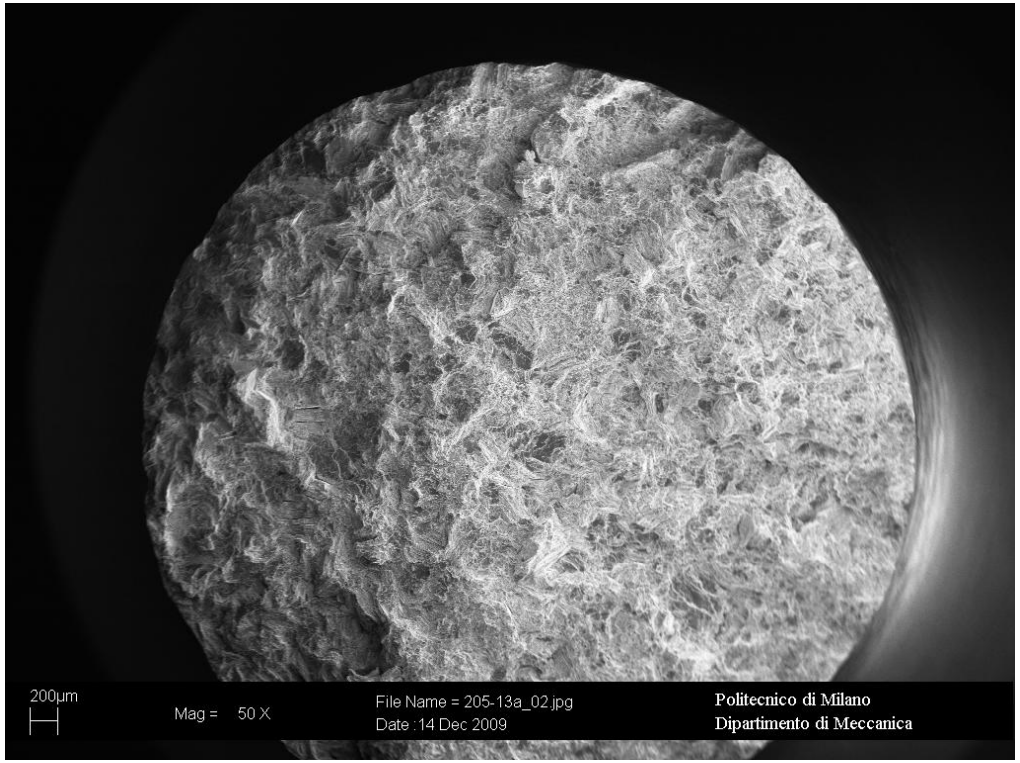

Specimen S/N: **205-13**

Applied stress range: 160 MPa

Loading ratio: R=0.6

Maximum stress: 400 MPa

Minimum stress: 240 MPa

Number of cycles to failure: 16584000 cycles

SEM analysis: tests at R=0.6 (704°C) (2)

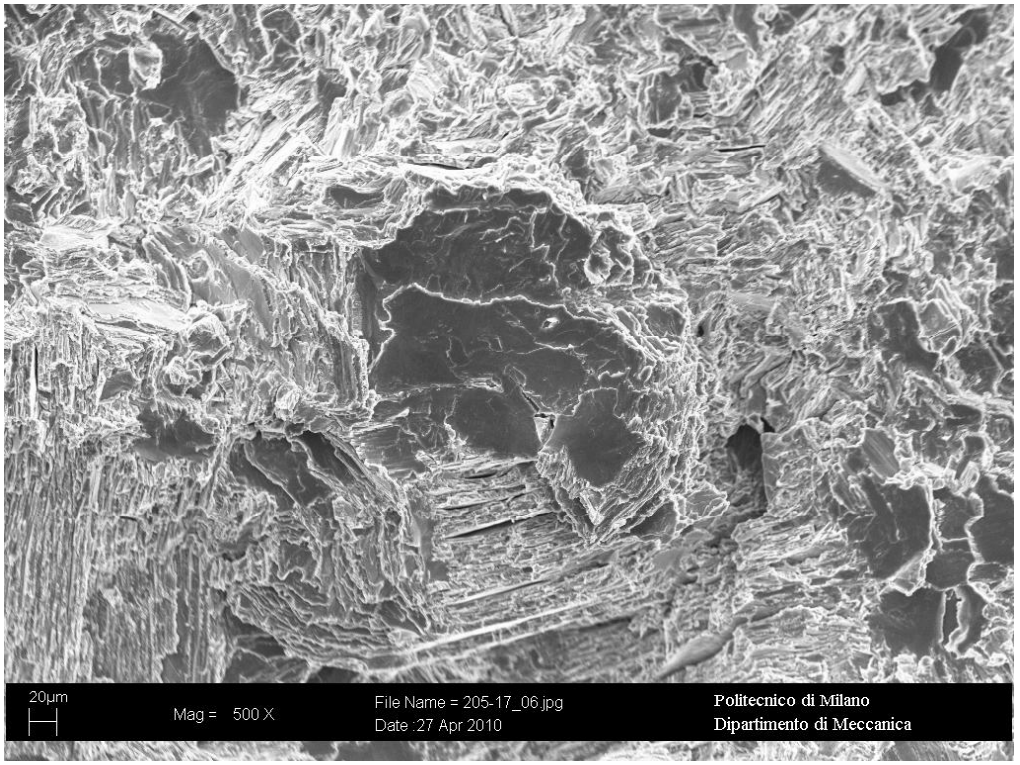

Specimen S/N: **205-17**

Applied stress range: 160 MPa

Loading ratio: R=0.6

Maximum stress: 400 MPa

Minimum stress: 240 MPa

Number of cycles to failure: 23.7 10^6 cycles

Microstructural features vs “defects”

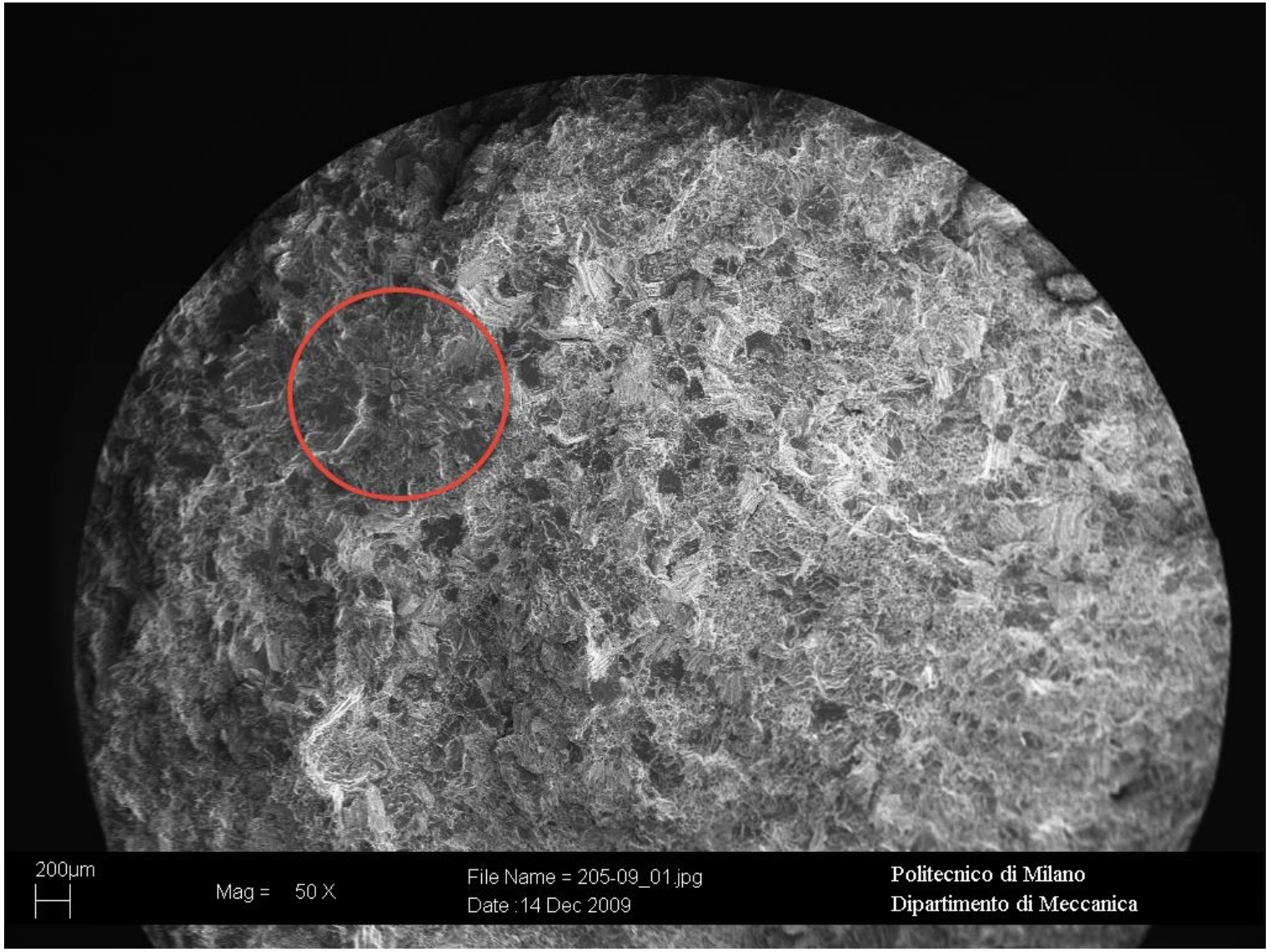

SEM analysis: tests at R=0 (704°C)

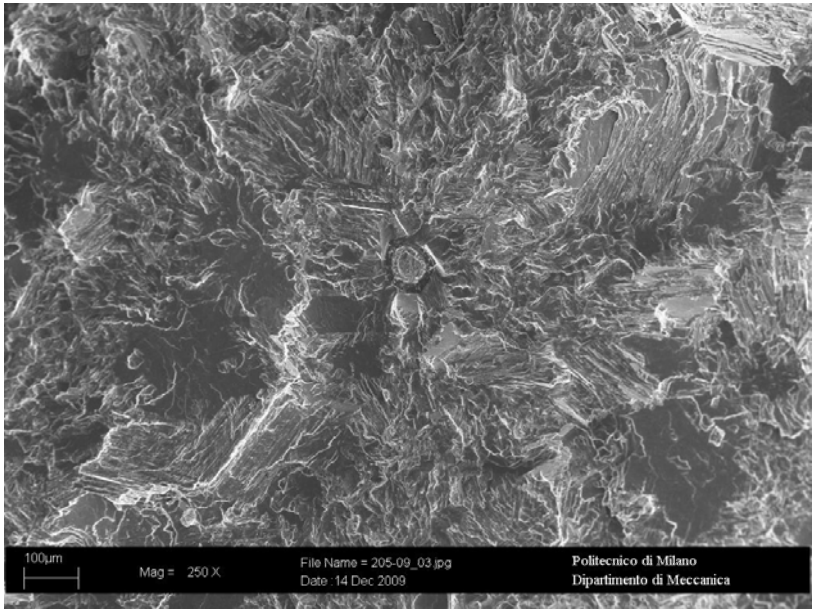

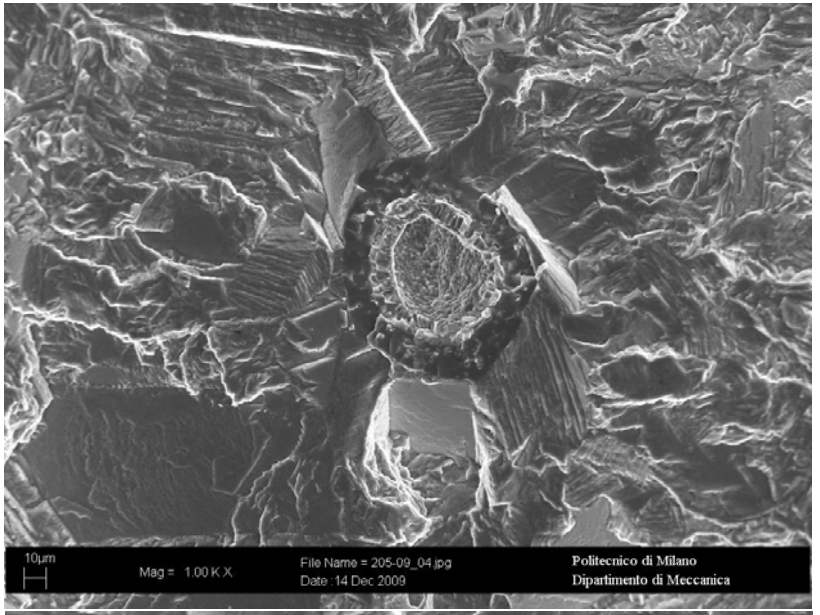

Applied stress range: 380 MPa

Loading ratio: R=0

Maximum stress: 380 MPa

Minimum stress: 0 MPa

Number of cycles to failure: 6975500 cycles

Area of defect: 7160 µm^2

Modelling defects

In one single case, a small process defect (area=7160 μm^2) caused subcritical crack growth under high stress σ_{max}=380 MPa, up to a “fish-eye” area of about 1.27 mm^2, corresponding to:

$K_{max} = 0.5\sigma_{max} \sqrt{(\pi\sqrt{area})} =$
$=11.3MPa\sqrt{m}$

in agreement with the Kmax value obtained in FCG tests.

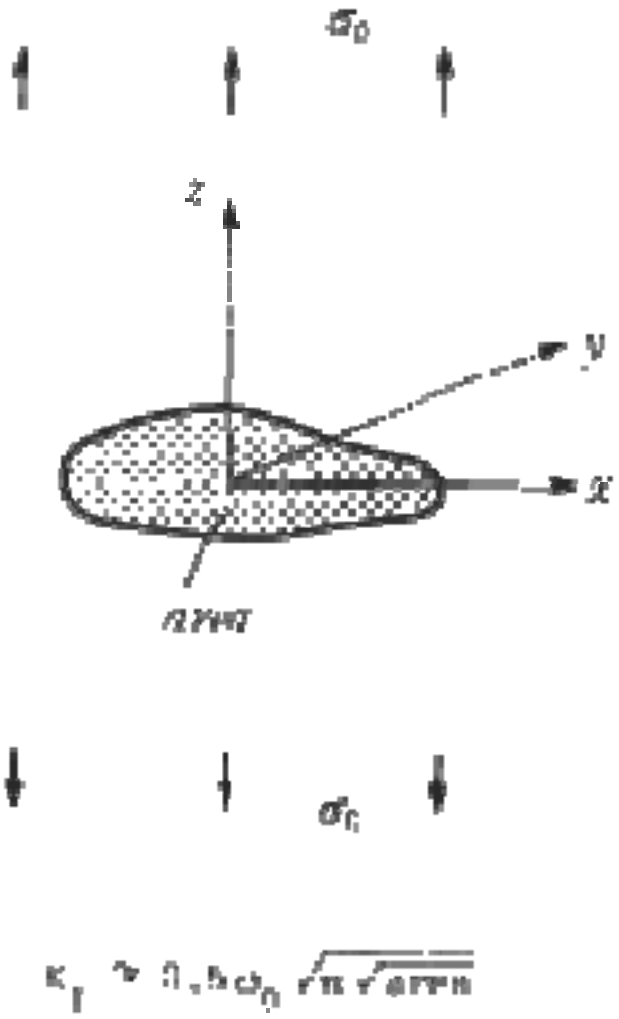

Conclusions

A potential disadvantage to cast and PM γ-TiAl alloys, in terms of component design, is their limited fatigue crack growth resistance compared to nickel-based superalloys.

In general, there is a small difference between the fatigue threshold stress-intensity-range of long cracks and the apparent fracture toughness, leading to shortened lifetimes for small changes in applied stress, should the fatigue threshold be exceeded.

On the other hand, in the case of the Ti-48Al-2Cr-2Nb alloy examined in this work, the advantage of the γ-TiAl produced by the EBM process is that typical defects of cast or PM materials can be avoided and higher fatigue threshold and fatigue strength respect to competing technologies can be obtained.

The experimentally observed fatigue properties give confidence in the application of EBM Ti-48Al-2Cr-2Nb to LPT blades.

Potential application also for HPC blading, thanks to superior fatigue performance of the studied material.